



Magnetic scattering with coherent X-ray beams: state of the art and perspectives

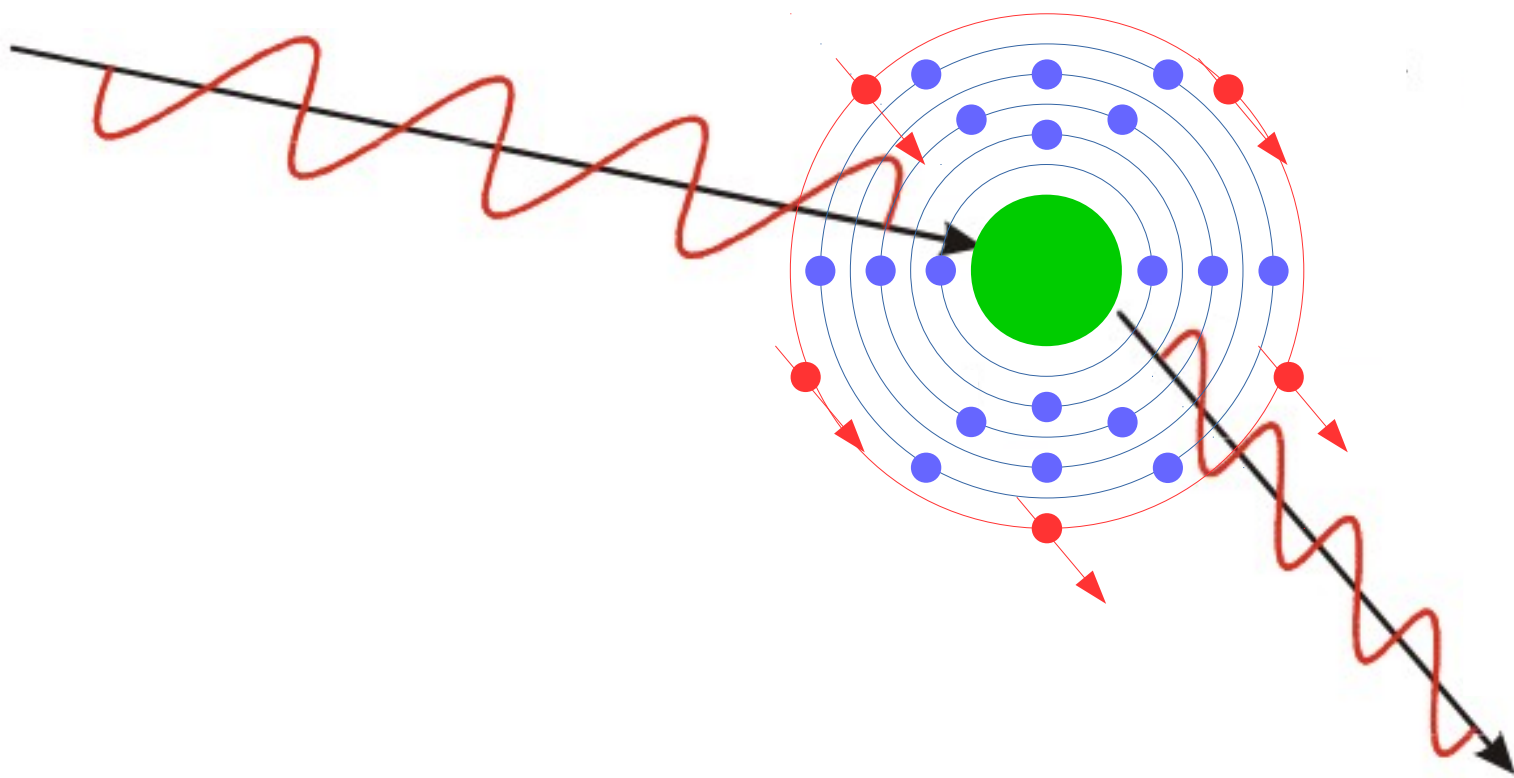
Guillaume Beutier

SIMaP, CNRS / Univ Grenoble Alpes / Grenoble INP, Grenoble, France

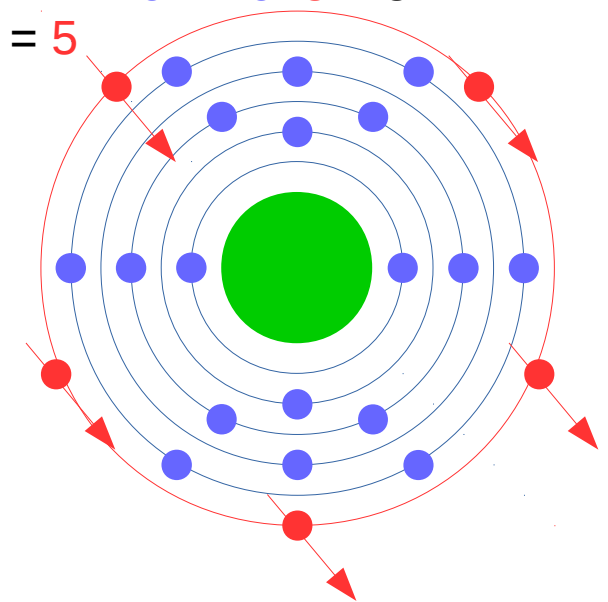
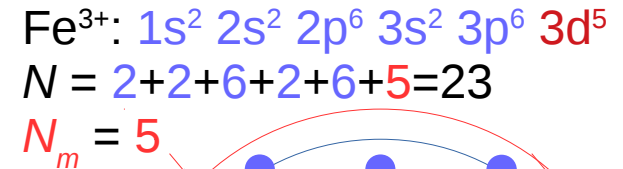


- 1) X-ray magnetic scattering
- 2) History of magnetic scattering with coherent x-ray beams of 3rd generation synchrotron facilities
 - magnetic speckles
 - XPCS (against time and magnetic field)
 - imaging
- 3) Perspectives with new synchrotron sources

X-ray magnetic scattering



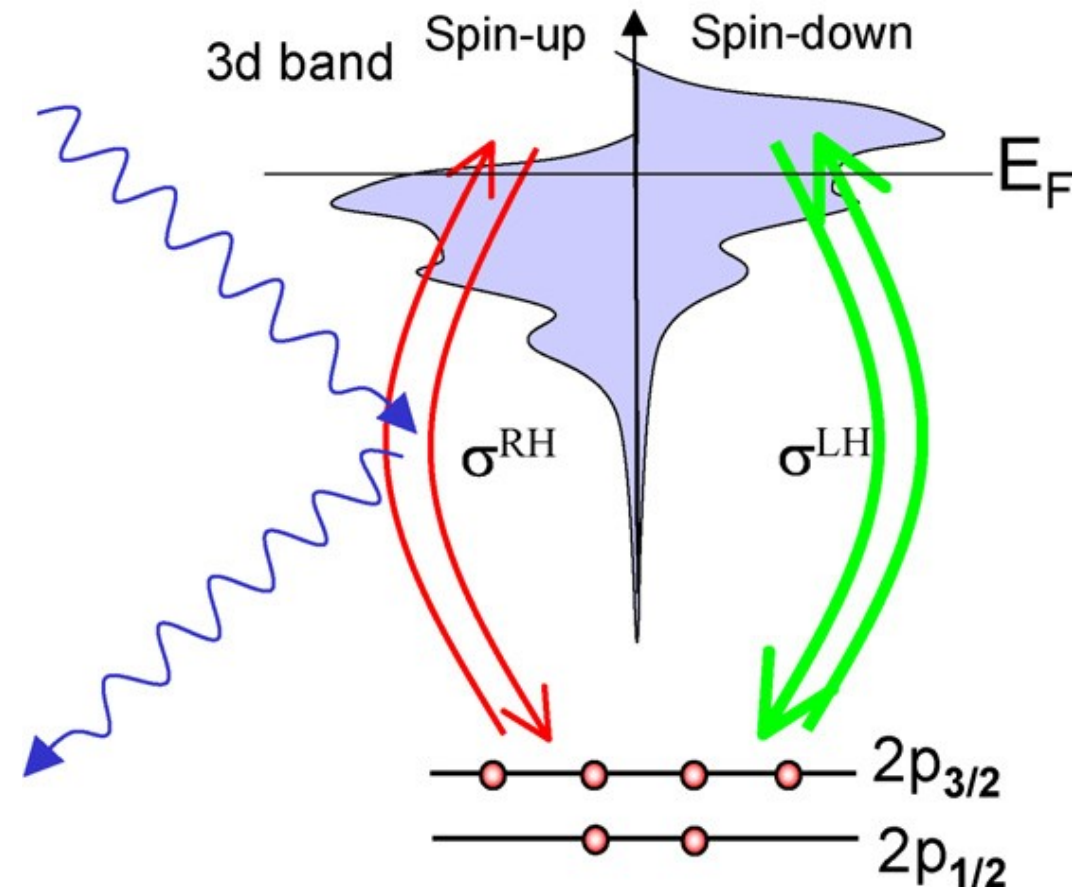
X-ray magnetic scattering



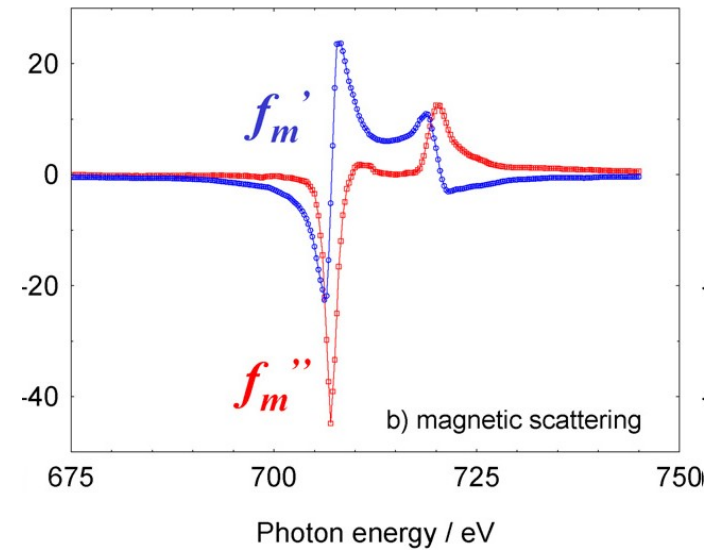
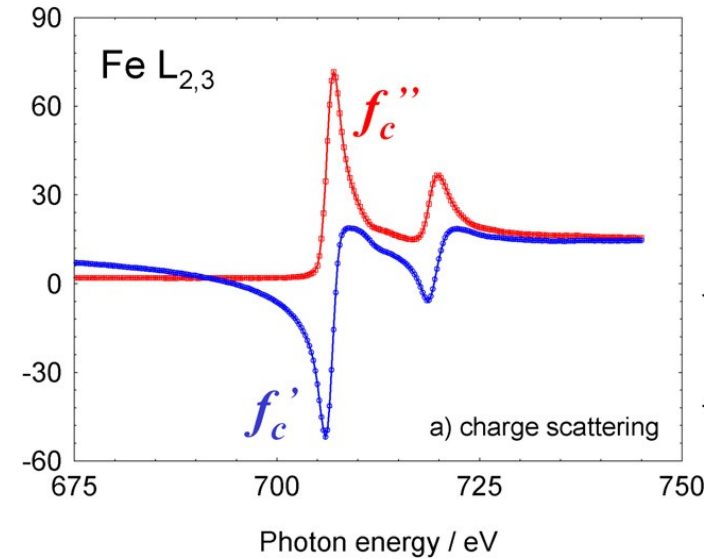
- Thomson scattering: measures electronic density
amplitude $\sim N$ (in r_0 units)
- Magnetic scattering: measures magnetic moments
- X-ray non-resonant magnetic scattering
amplitude $\sim \hbar\omega/511\text{keV} N_m \sim 0.001 - 0.01 N_m$
→ too weak to be used with a “weak” coherent beam
(1 exception: SDW in Cr: Jacques *et al*, Eur. Phys. J. B 70, 317–325 (2009))
- X-ray resonant magnetic scattering (XRMS):
enhancement of magnetic scattering by exciting a virtual electronic transition
- UAs: antiferromagnetic order → pure magnetic reflections
(Isaacs *et al*, Phys. Rev. Lett. **62**, 1671, (1989))
 - intensity of magnetic reflections **enhanced by 7 orders of magnitude** at U M_{IV} edge
 - resonant magnetic intensity $\sim 1\%$ of structural reflection (0,0,2)
→ magnetic scattering amplitude $\sim 9r_0$

X-ray Resonant Magnetic Scattering (XRMS)

Virtual transitions between 2p and 3d states



⇒ chemical selectivity
⇒ shell selectivity



G. van der Laan, C.R. Physique 9, 570 (2008)

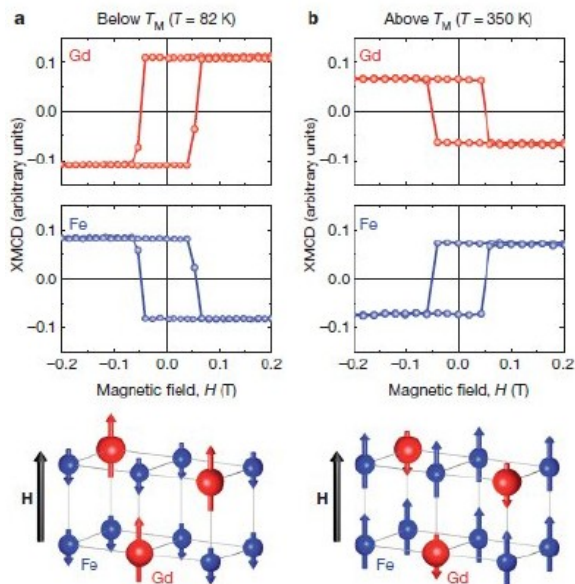
X-ray Resonant Magnetic Scattering (XRMS)

Series	Abs. edge	Energy (keV)	λ (Å)	Shells	Type	Resonant amplitude (r_0 units)
3d "common" transition metals	$L_{2,3}$	0.4–1.0	12–30	$2p \rightarrow 3d$	E1	≈ 1.00
	K	4.5–9.5	1.3–2.7	$1s \rightarrow 4p$	E1	≈ 0.02
				$1s \rightarrow 3d$	E2	≈ 0.01
5d Re, Os, Ir, Pt	$L_{2,3}$	5.4–14	0.9–2.2	$2p \rightarrow 5d$	E1	≈ 1.00
4f rare-earth	$L_{2,3}$	5.7–10.3	1.2–2.2	$2p \rightarrow 5d$	E1	≈ 0.10
				$2p \rightarrow 4f$	E2	≈ 0.05
	$M_{4,5}$	0.9–1.6	7.7–13.8	$2d \rightarrow 4f$	E1	≈ 100
5f uranides	$L_{2,3}$	17–21	0.6–0.7	$2p \rightarrow 6d$	E1	≈ 0.05
				$2p \rightarrow 4f$	E2	≈ 0.01
	$M_{4,5}$	3.5–4.5	2.7–6	$3d \rightarrow 5f$	E1	≈ 10.0

L. Paolasini & F. de Bergevin / C. R. Physique **9** (2008) 550–569

X-ray Resonant Magnetic Scattering – main applications

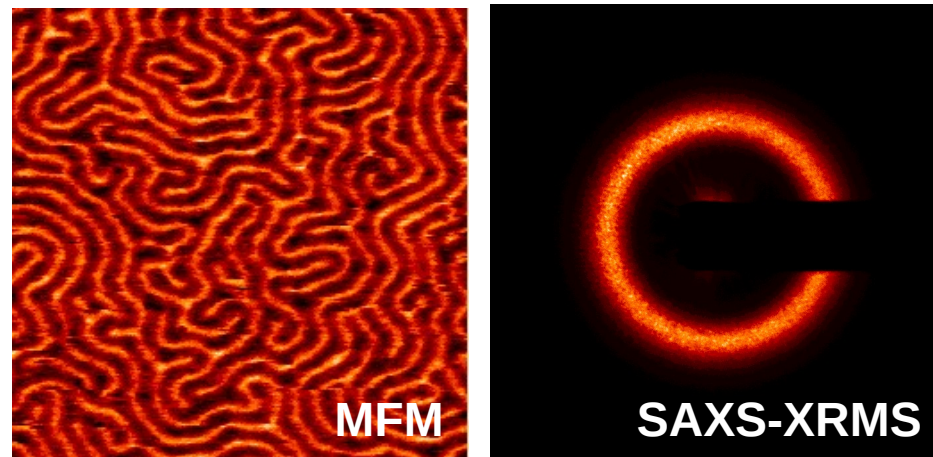
Transmission / Absorption (XMCD)



Ferrimagnetic alloy

Radu *et al*, Nature **472**, 205 (2011)

SAXS → domain size, short range order

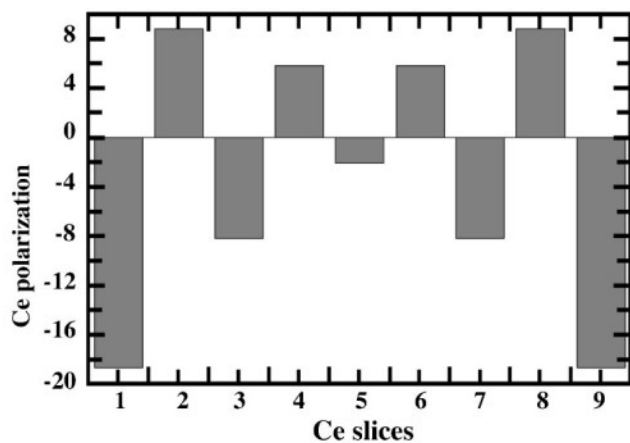


FeGd thin film showing a maze of up and down magnetization domains

Miguel *et al*, Phys. Rev. B **74**, 094437 (2006)

Reflectivity (XRMR)

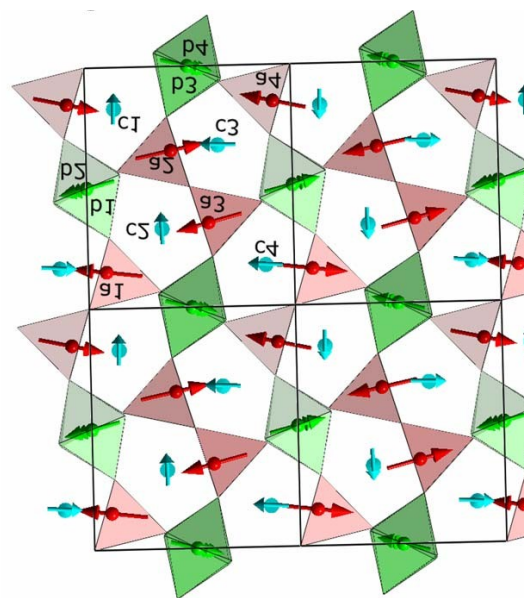
→ in-depth magnetisation profile in thin films and multilayers (coupling, roughness...)



$(\text{Ce}_{22\text{\AA}}/\text{Fe}_{30\text{\AA}})_{50}$

Sève *et al*, PRB 1999

Diffraction → crystallographic magnetic structure



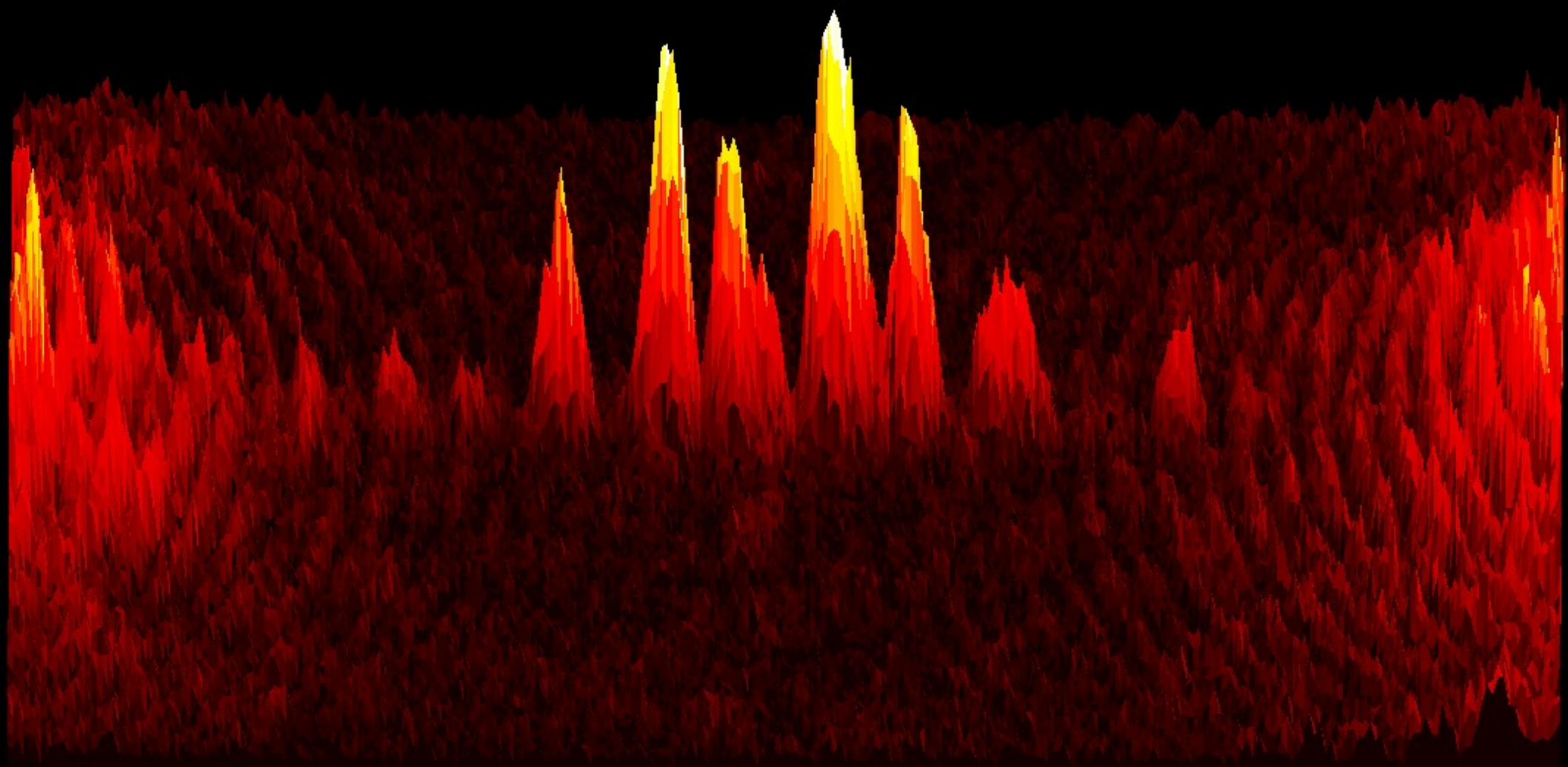
- Neutron absorbing elements (Gd, ...)
- Several magnetic elements
- Small crystals
- Need high resolution

RMn_2O_5 multiferroics

Beutier *et al*, PRB 2008

Lee *et al*, PRL 2013

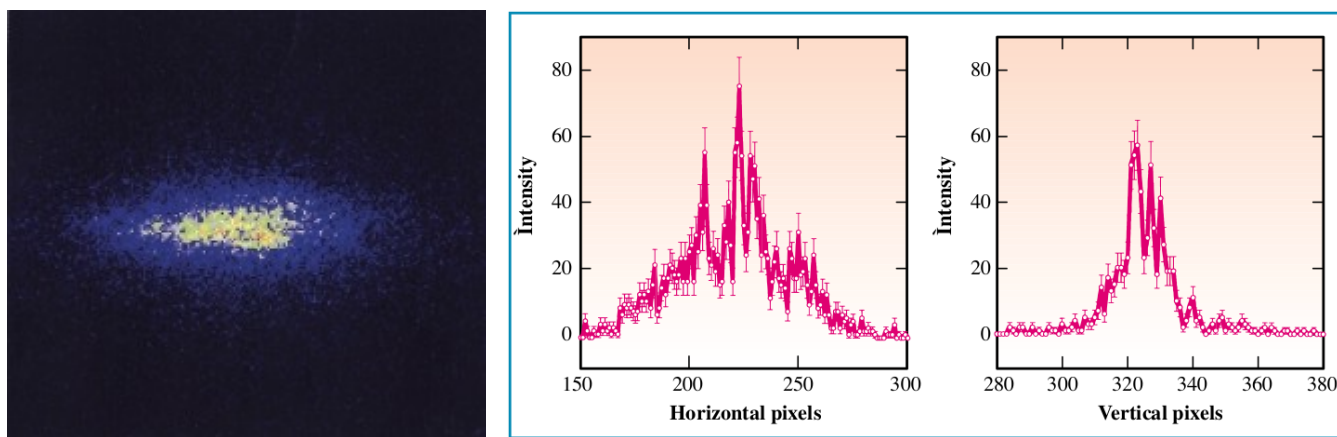
Magnetic speckles



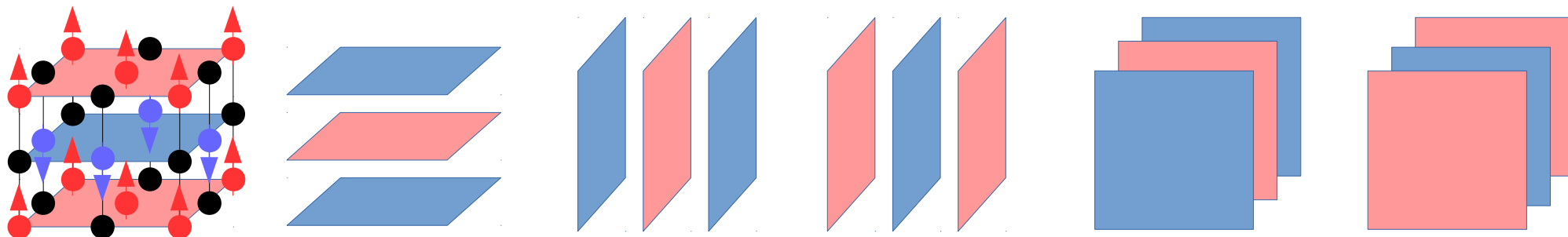


FIRST OBSERVATION OF A MAGNETIC SPECKLE PATTERN BY COHERENT X-RAY SCATTERING AT THE URANIUM M_{IV} EDGE

F. YAKHOU¹, A. LÉTOUBLON², F. LIVET², M. DE BOISSIEU², F. BLEY² AND C. VETTER¹



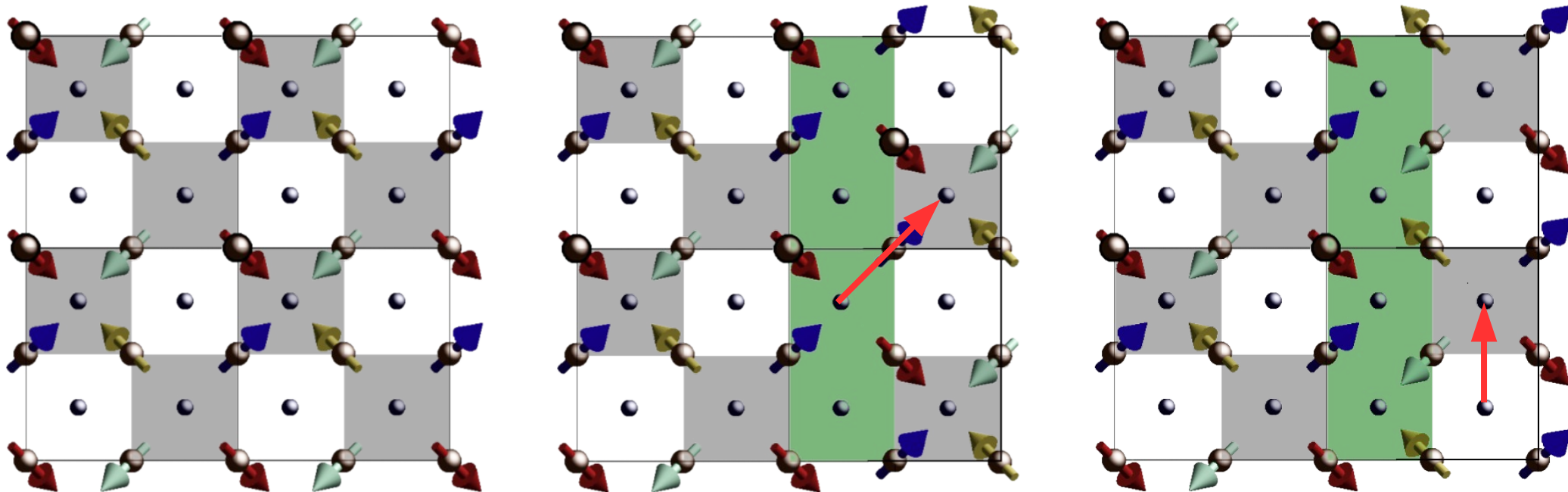
(001) magnetic reflection of UAs, U M_{IV} edge (3.73 keV), ESRF ID20



Later published in Yakhou et al. / Journal of Magnetism and Magnetic Materials 233 (2001) 119

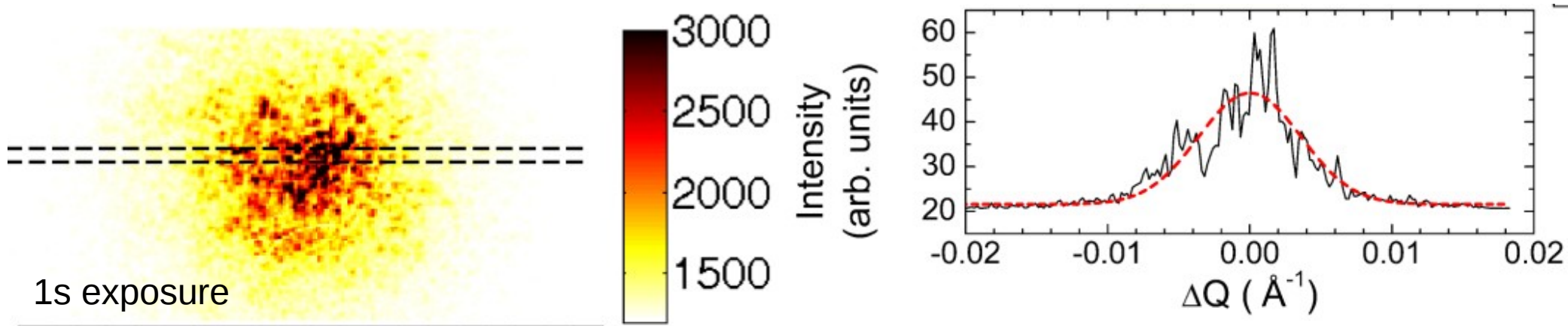
Magnetic speckles

USb: cubic system with triple-k magnetic structure → “all-in” / “all-out” local configurations



(003) magnetic Bragg reflection, U M_4 edge (3.728 keV)

Diamond Light Source beamline I16

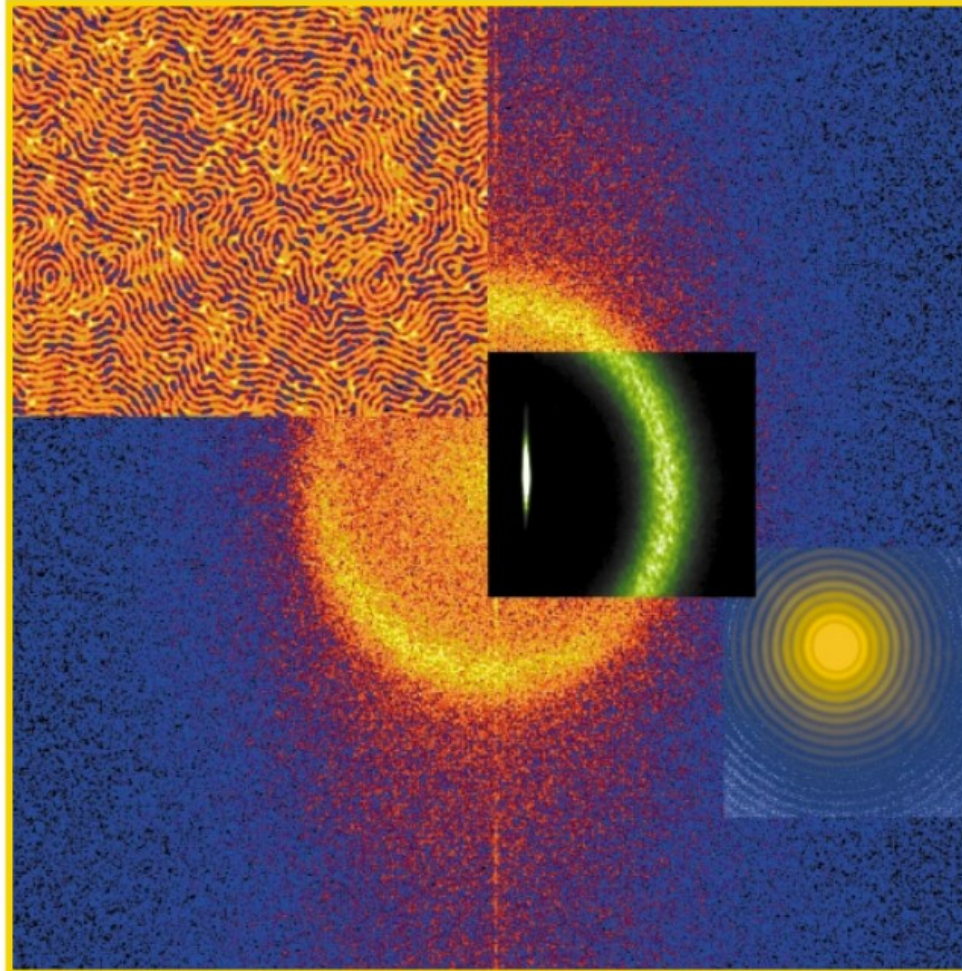


Lim *et al*, Journal of Physics: Conference Series **519** (2014) 012010



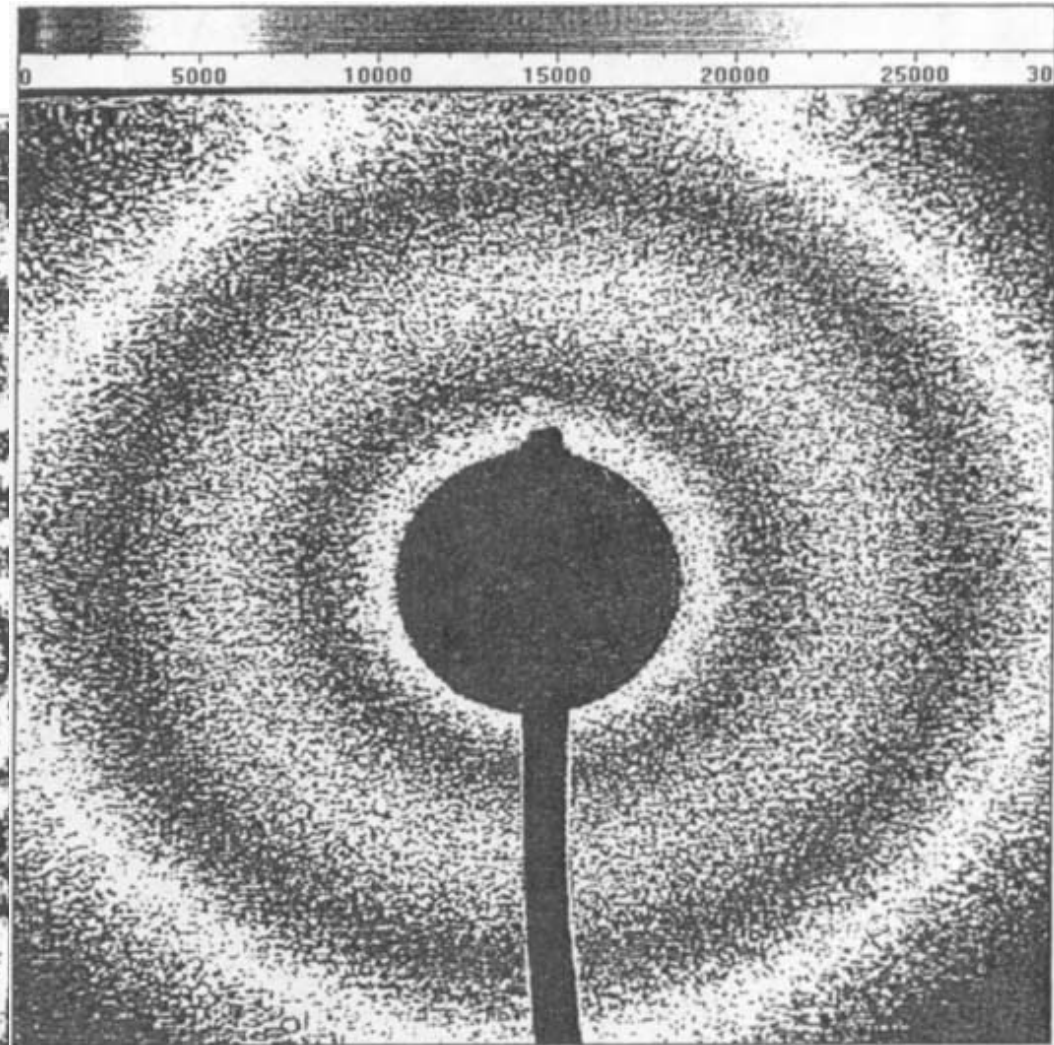
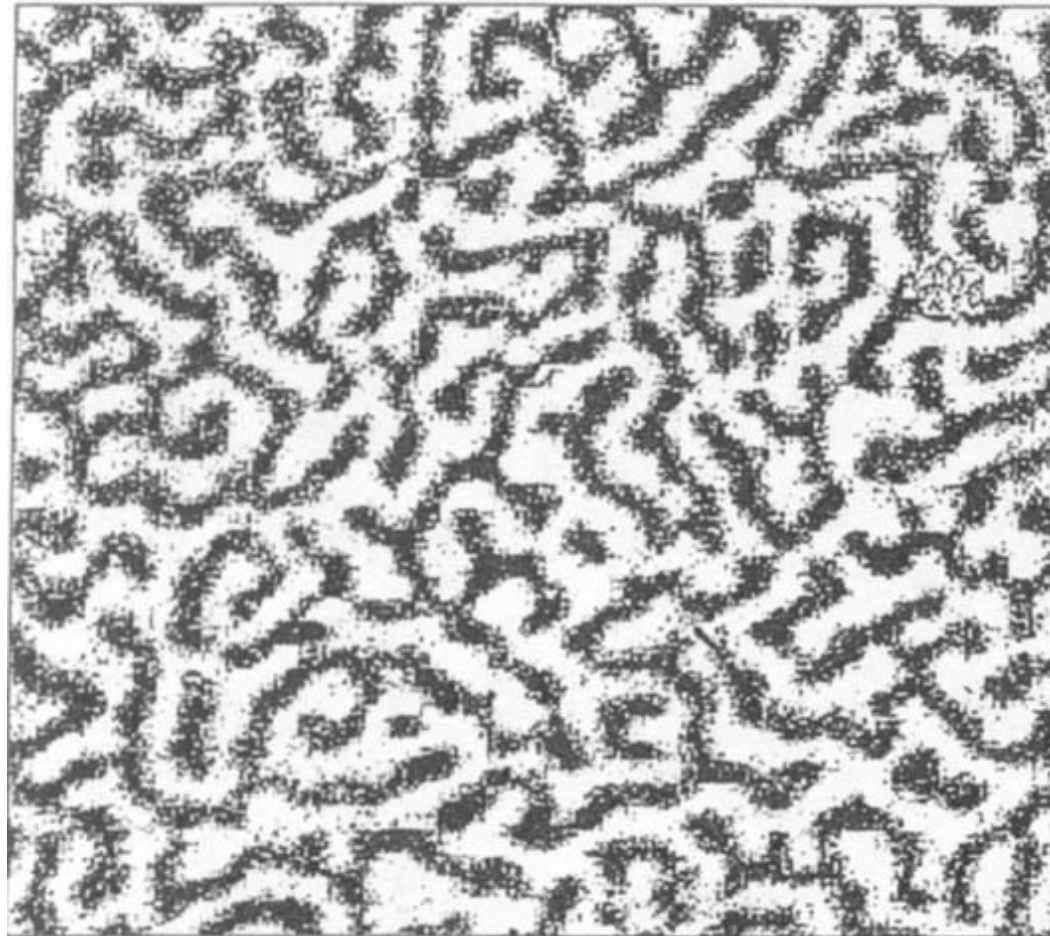
MAGNETIC SPECKLES WITH SOFT X-RAYS

J.F. PETERS, M.A. DE VRIES, J. MIGUEL, O. TOULEMONDE AND J.B. GOEDKOOP



A Magnetic Force Microscopy image of the magnetic domains in GdFe_2 thin films (top left); the diffraction image from these domains as taken on beamline ID12B (centre); and a Fraunhofer image illustrating the nearly perfect coherence that can be obtained with soft X-rays (bottom right). In the background is the 2-D powerspectral density of the MFM picture.

Magnetic speckles

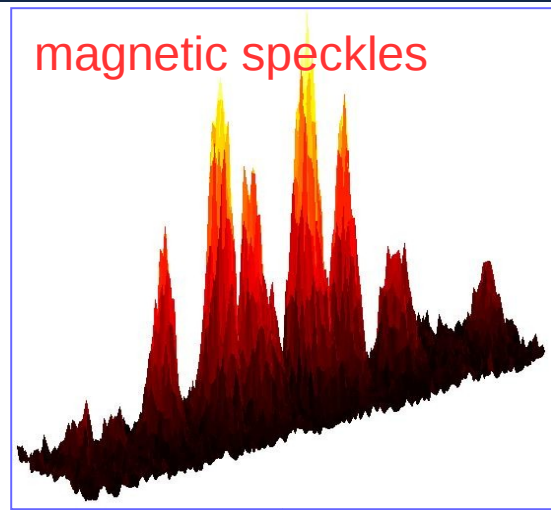


Co/Pt multilayer, transmission X-ray microscope

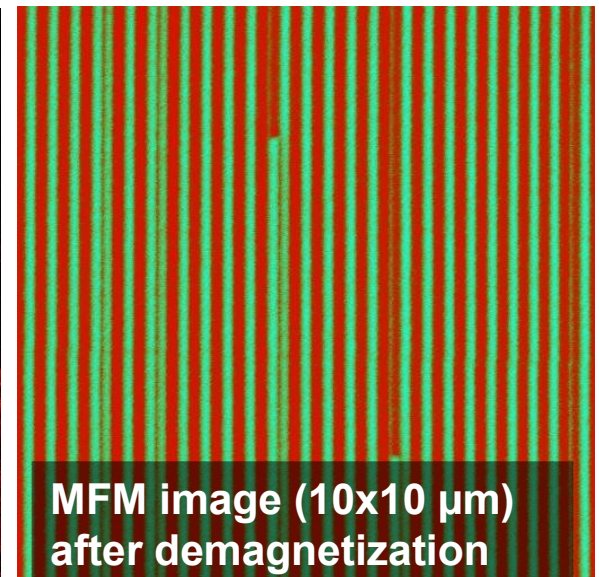
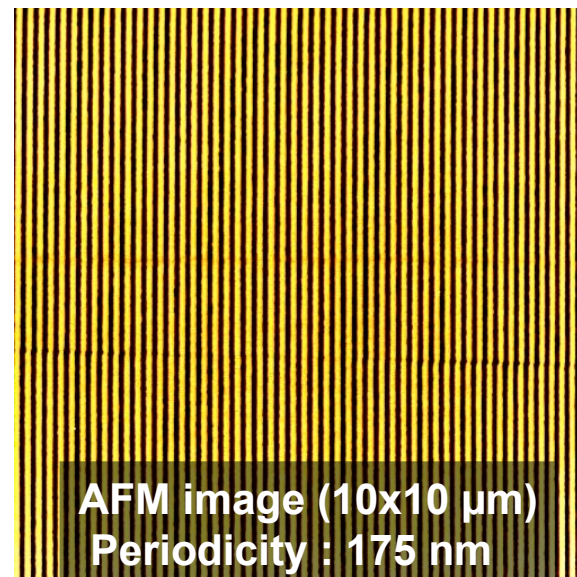
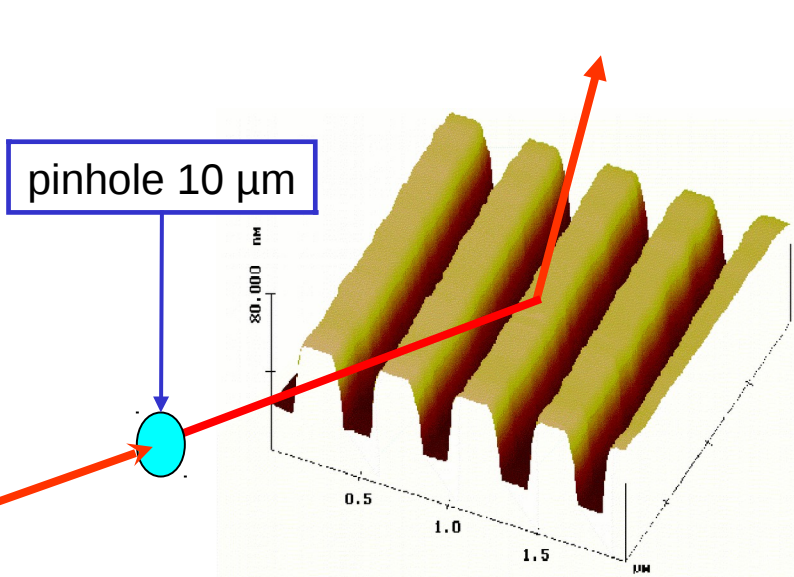
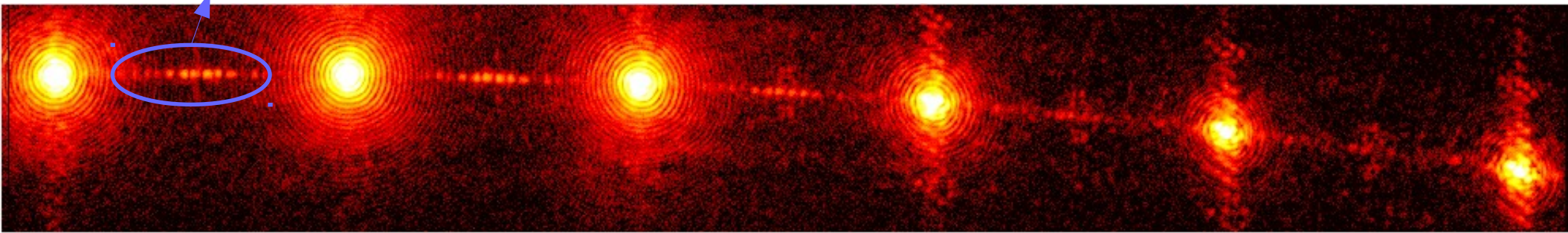
Coherent soft XRMS pattern on CCD

Coherent soft X-ray magnetic scattering,
Bo Hu, Phillip Geissbuhler, Larry Sorensen, Stephen D. Kevan, Jeffrey B. Kortright & Eric E. Fullerton
Synchrotron Radiation News, 14, 11-19 (2001)

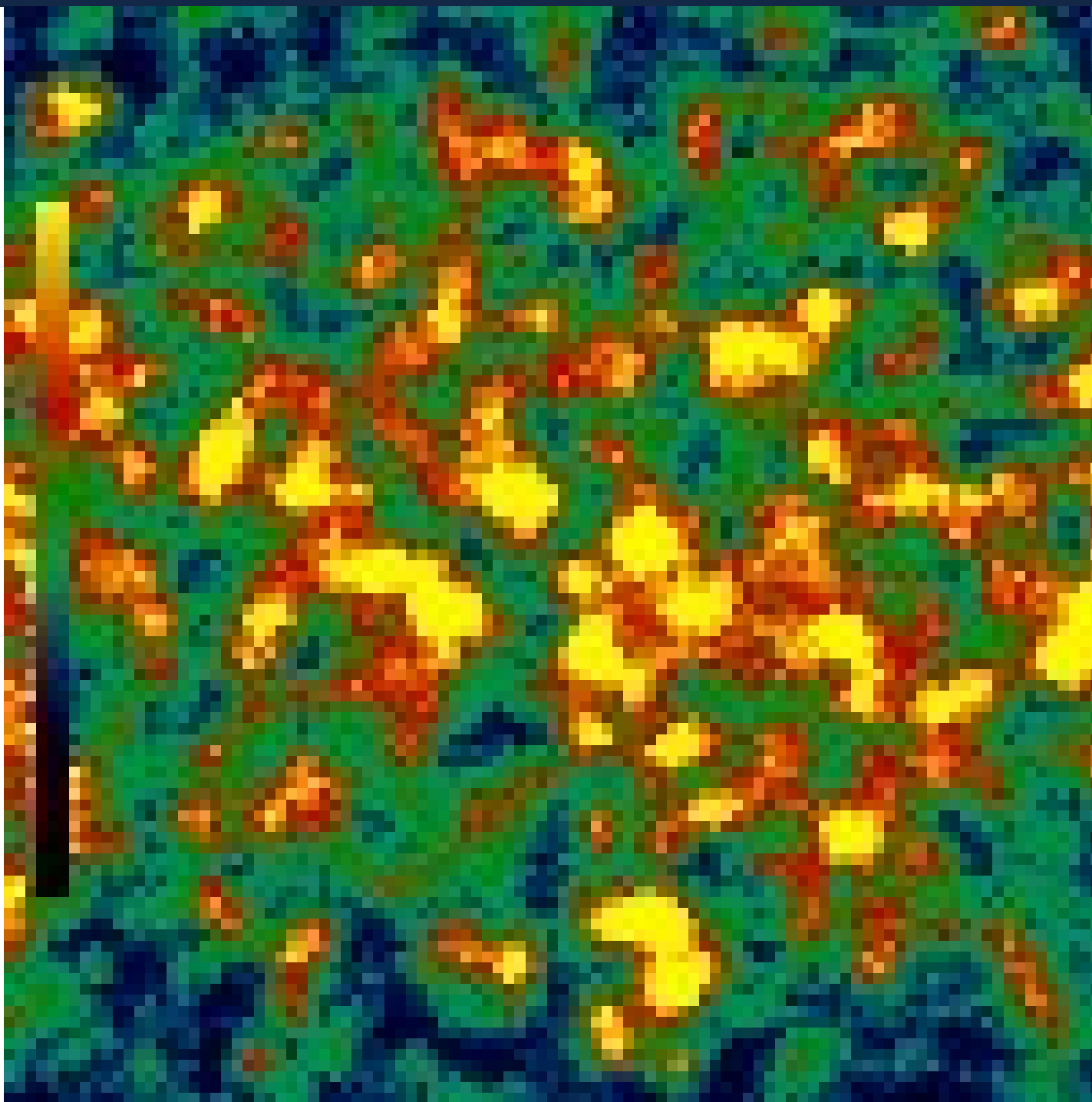
Magnetic speckles



ESRF ID08 (2004)
Co L_3 edge (778 eV)
Si grating covered with a Co/Pt multilayer



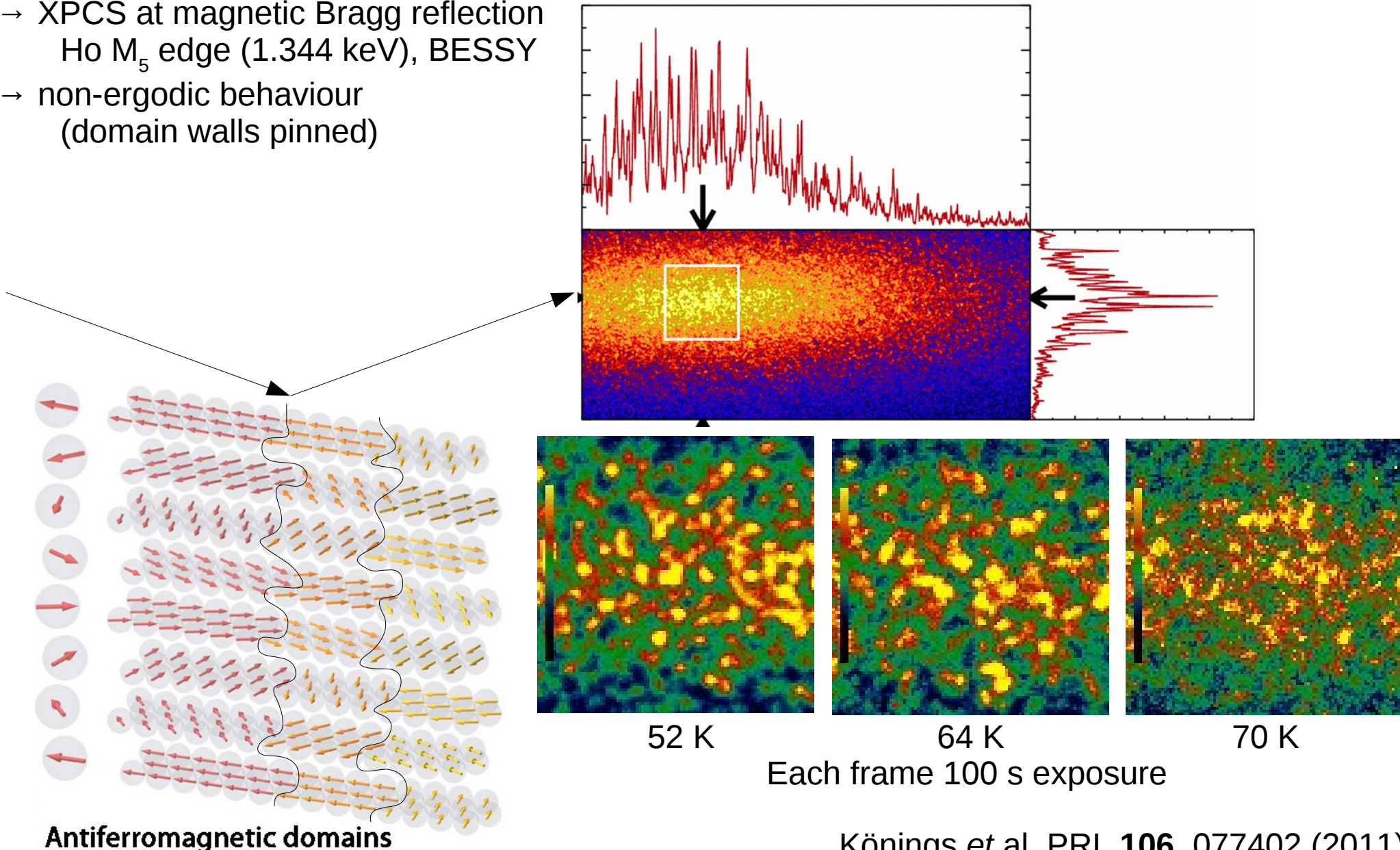
Magnetic XPCS



Magnetic XPCS

Antiferromagnetic domain fluctuations in Ho ultrathin film (helical magnetic structure)

- XPCS at magnetic Bragg reflection
Ho M_5 edge (1.344 keV), BESSY
- non-ergodic behaviour
(domain walls pinned)



Könings *et al*, PRL **106**, 077402 (2011)
Similar study on Y/Dy/Y thick film: Chen *et al*, PRL **110**, 217201 (2013)

Magnetic XPCS

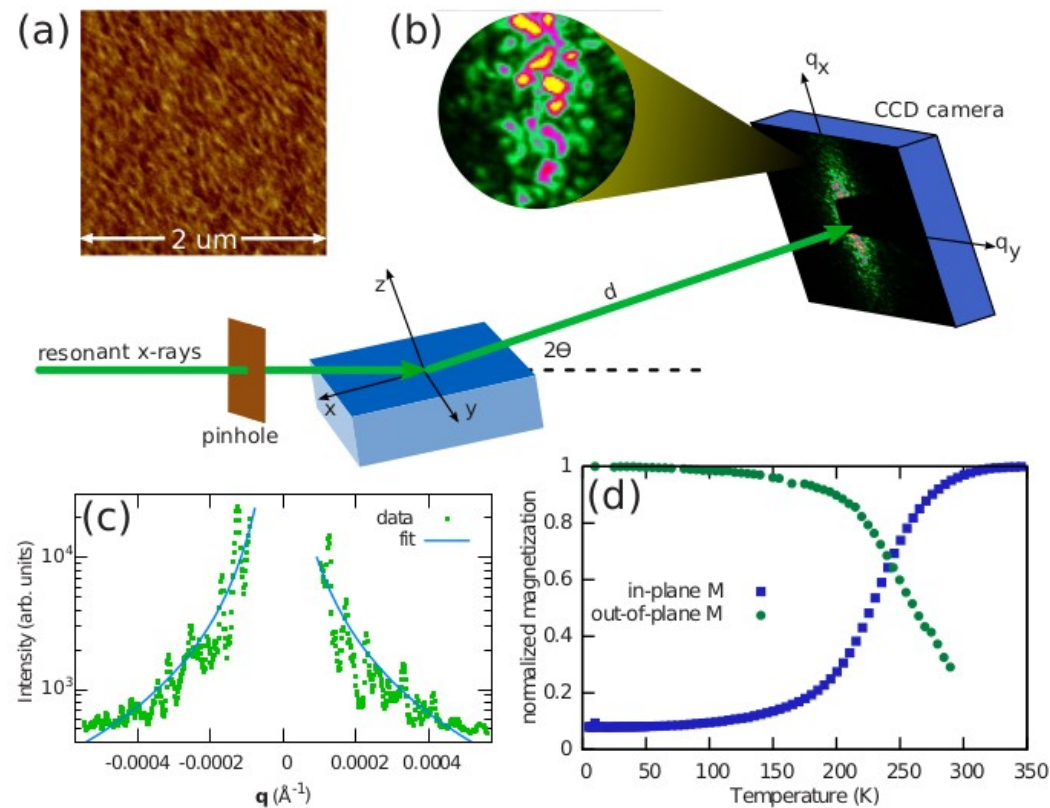


FIG. 1. (Color online) (a) MFM image of the sample at 300 K. The geometry for the resonant x-ray scattering experiment is shown in (b). Incident x-rays are filtered with a $\sim 10 \mu\text{m}$ pinhole, creating a spatially coherent light source. The scattering pattern is collected with a CCD camera at an angle of $2\theta=18^\circ$. Detail of the speckle pattern is shown in the inset. Line cut of the data is shown in (c). The spin reorientation of the sample is illustrated by the SQUID curves in (d), where the magnetization changes from out-of-plane to in-plane as the temperature is increased.

Cone phase and magnetization fluctuations in **Au/Co/Au** thin films near the spin-reorientation transition
 Seu *et al*, Phys. Rev. B **82**, 012404 (2010)

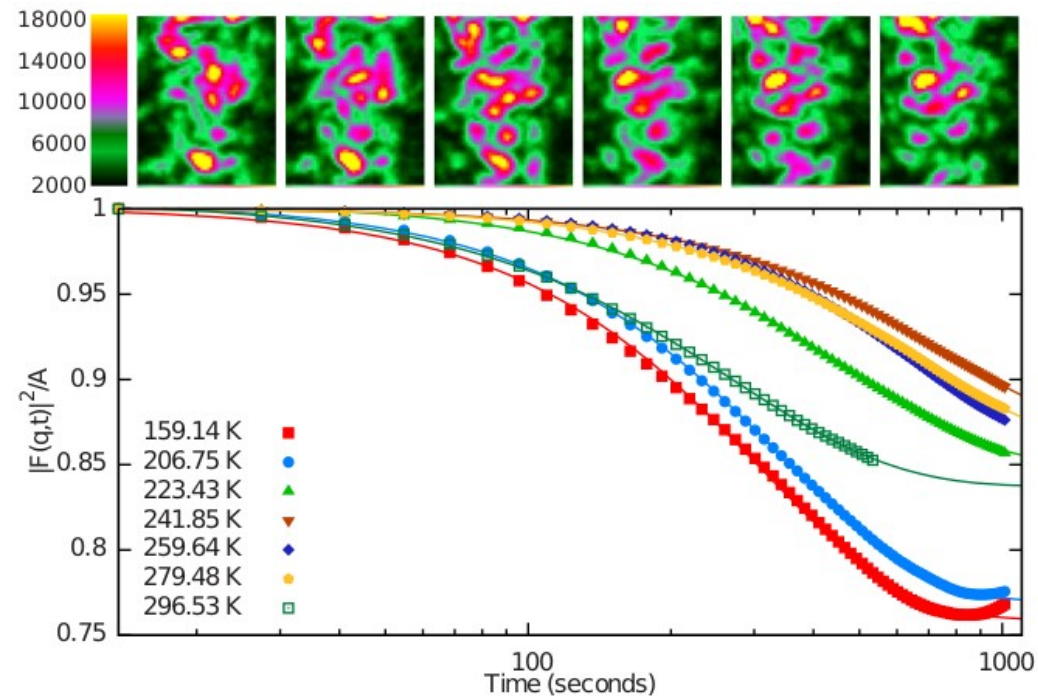


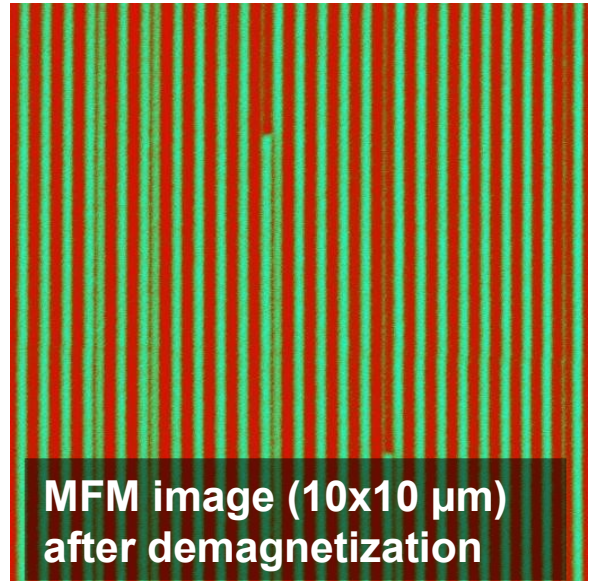
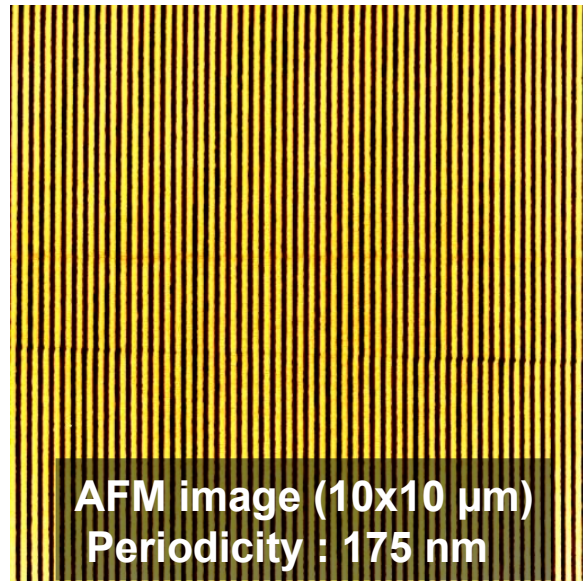
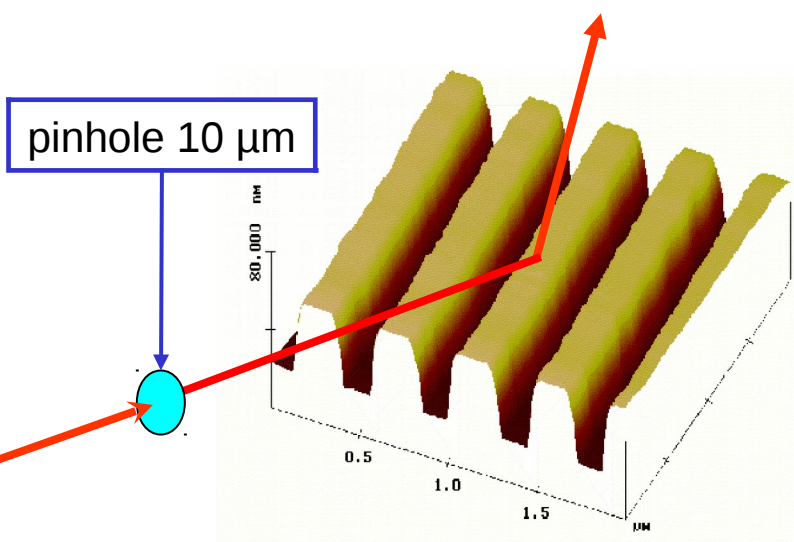
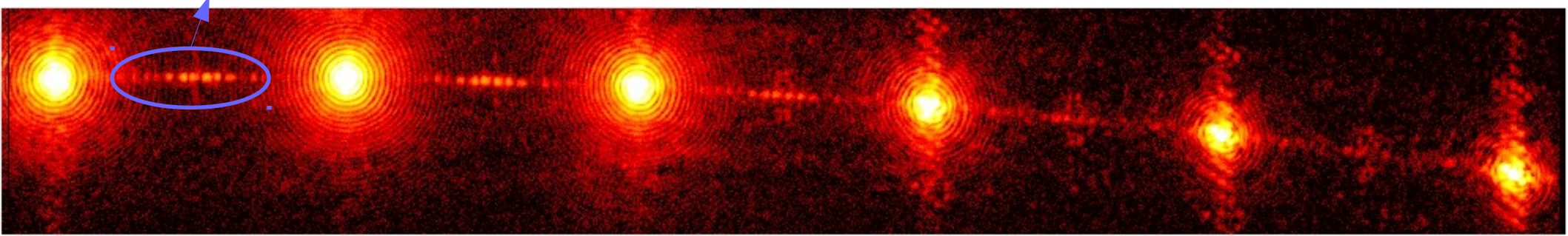
FIG. 2. (Color online) Top Panel: false color plot of the speckle pattern. The images are separated in time by 410.5 s. Plot of the intermediate scattering function $F(\mathbf{q}, t)$ as a function of temperature for $\mathbf{q}=2.58 \times 10^{-4} \text{ \AA}^{-1}$. The curves are normalized by the speckle contrast A . The lines are fits to the data. The form of the fit is a stretched exponential and is discussed in the text.

Magnetic XPCS / applied magnetic field

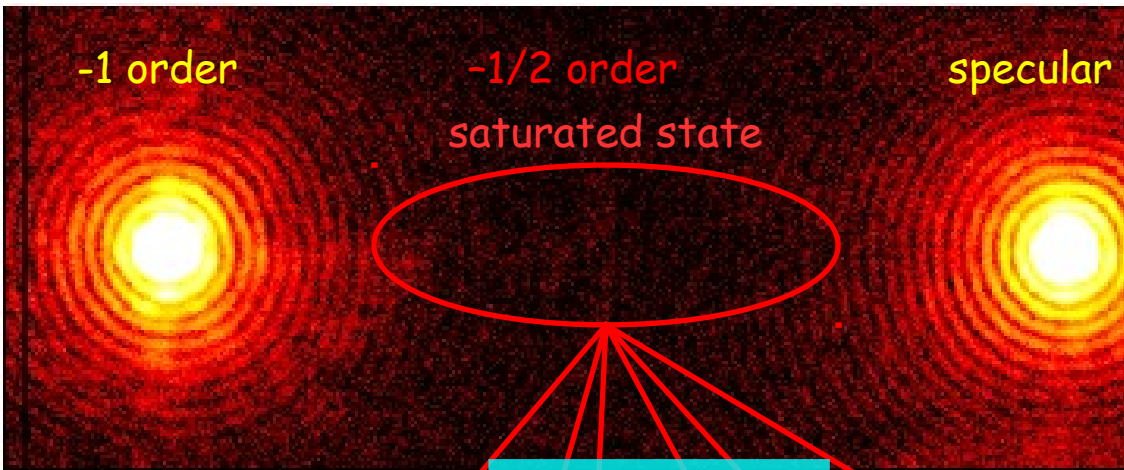
magnetic speckles

~1250 photons

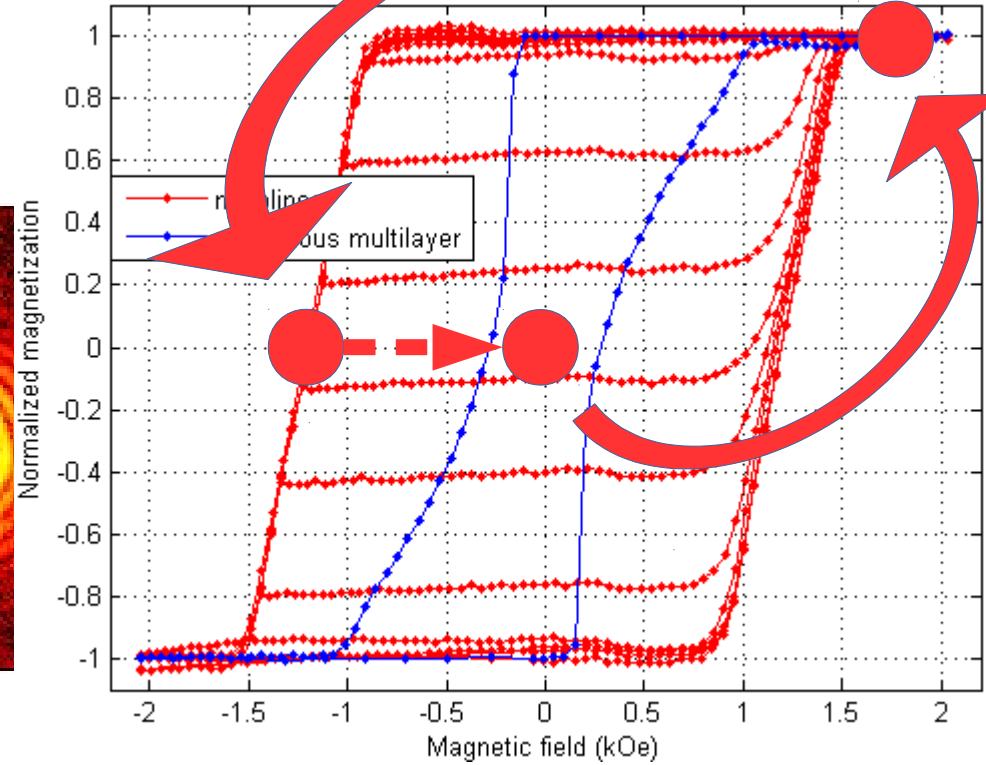
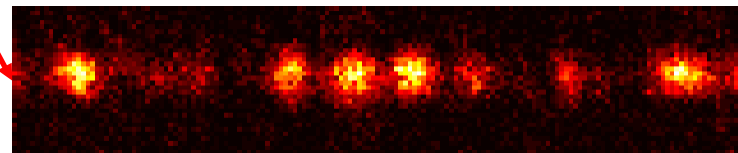
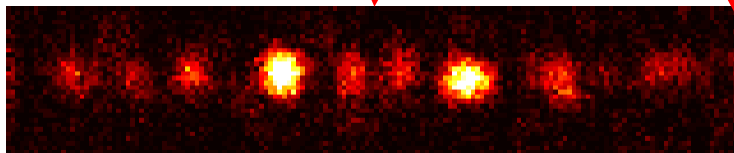
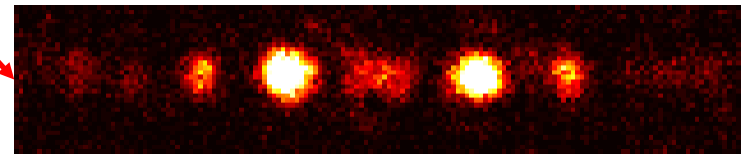
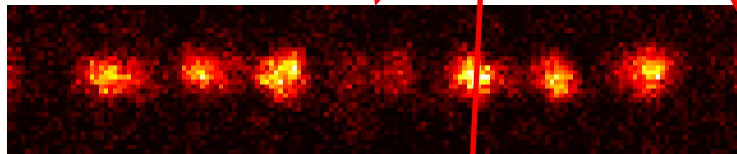
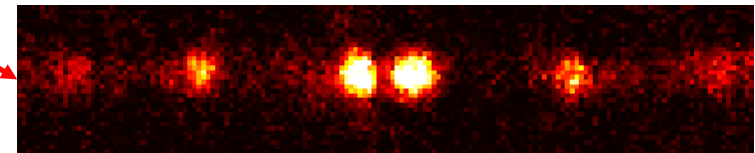
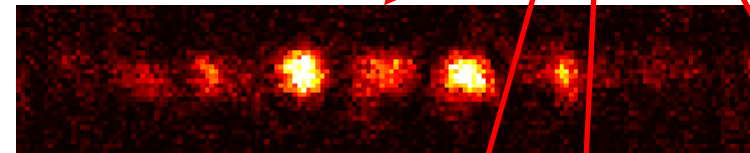
ESRF ID08 (2004)
Co L₃ edge (778 eV)
Si grating covered with a Co/Pt multilayer



Magnetic XPCS / applied magnetic field

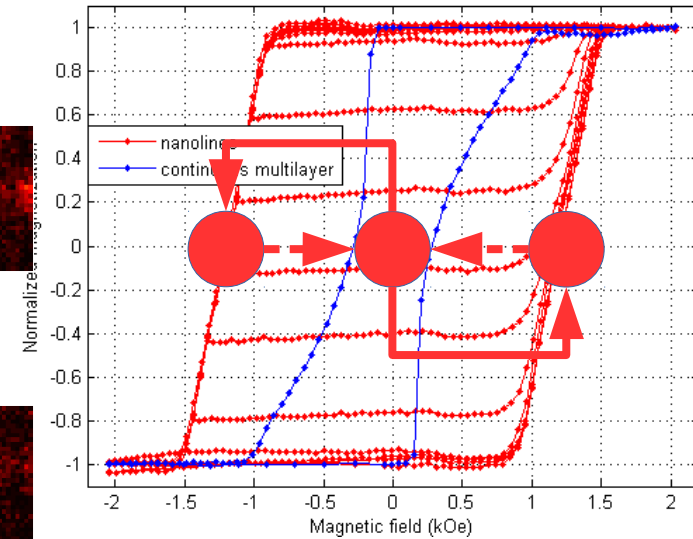
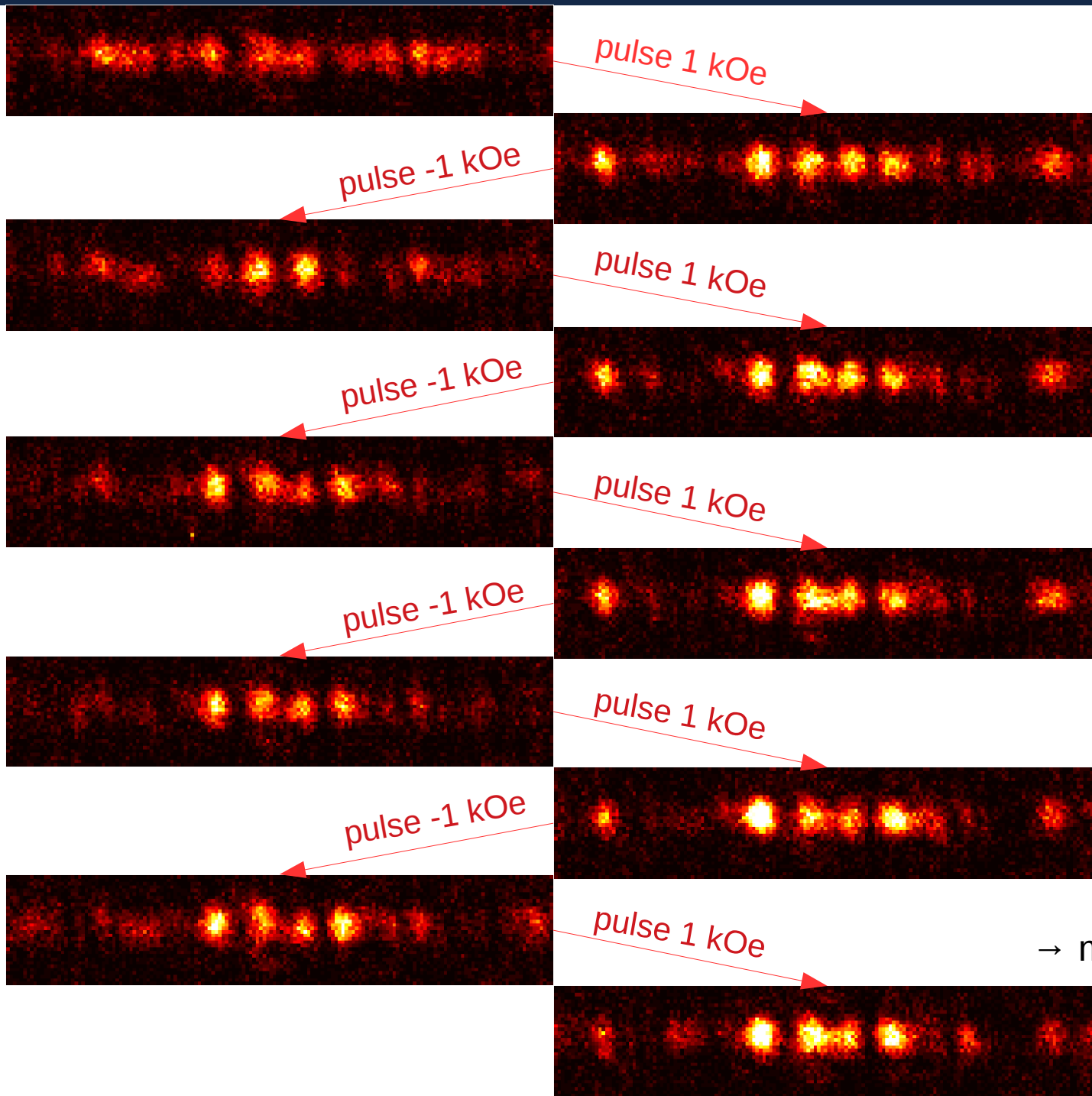


1 kOe - pulse
(coercive field)



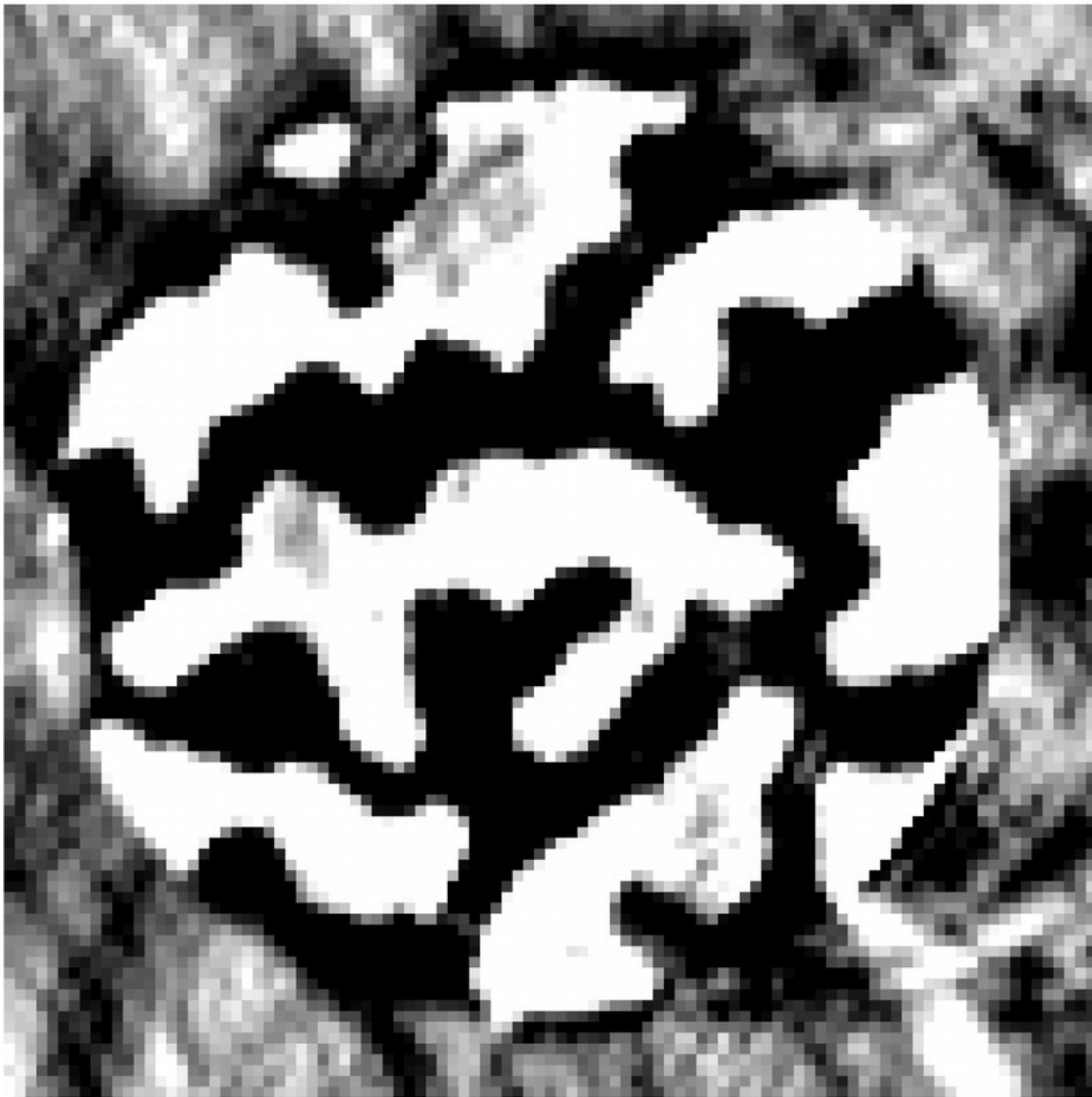
→ The magnetization reversal process from the saturated state is not reproducible

Magnetic XPCS / applied magnetic field



→ magnetic memory in minor loop
Beutier *et al*, New Journal of
Physics 11 (2009) 113026

Magnetic imaging



XRMS scattering factor:

$$f \rightarrow f^{res} = \underbrace{F^{(0)}(\hat{e}_f^* \cdot \hat{e}_i)}_{\text{charge scattering}} - \underbrace{iF^{(1)}(\hat{e}_f^* \wedge \hat{e}_i) \cdot \hat{m}}_{\text{magnetic scattering}}$$

charge scattering magnetic scattering

m : local magnetisation unit vector

\hat{e}_i : polarisation of incident photons

\hat{e}_f : polarisation of scattered photons

$$\rightarrow I = I_{\sigma} + I_{\pi}$$

→ **magnetic scattering is incompatible with CDI**

Ways to get rid of charge scattering:

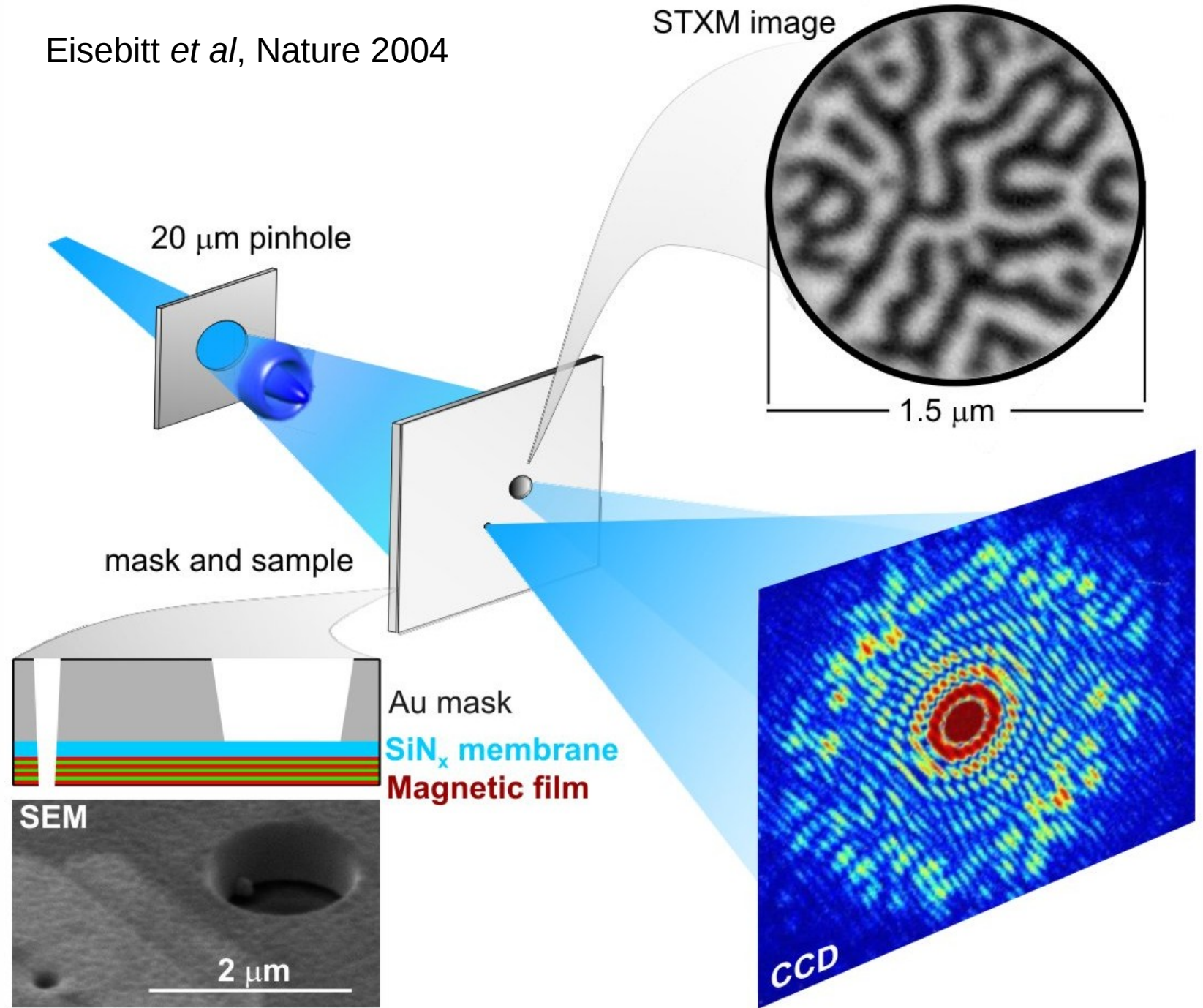
- Magnetic signal is in region of reciprocal space with no charge scattering
- Subtraction of a non-magnetic state
- Polarisation analysis
- Circular dichroism (ferromagnets)
- Ptychography

CDI hypothesis

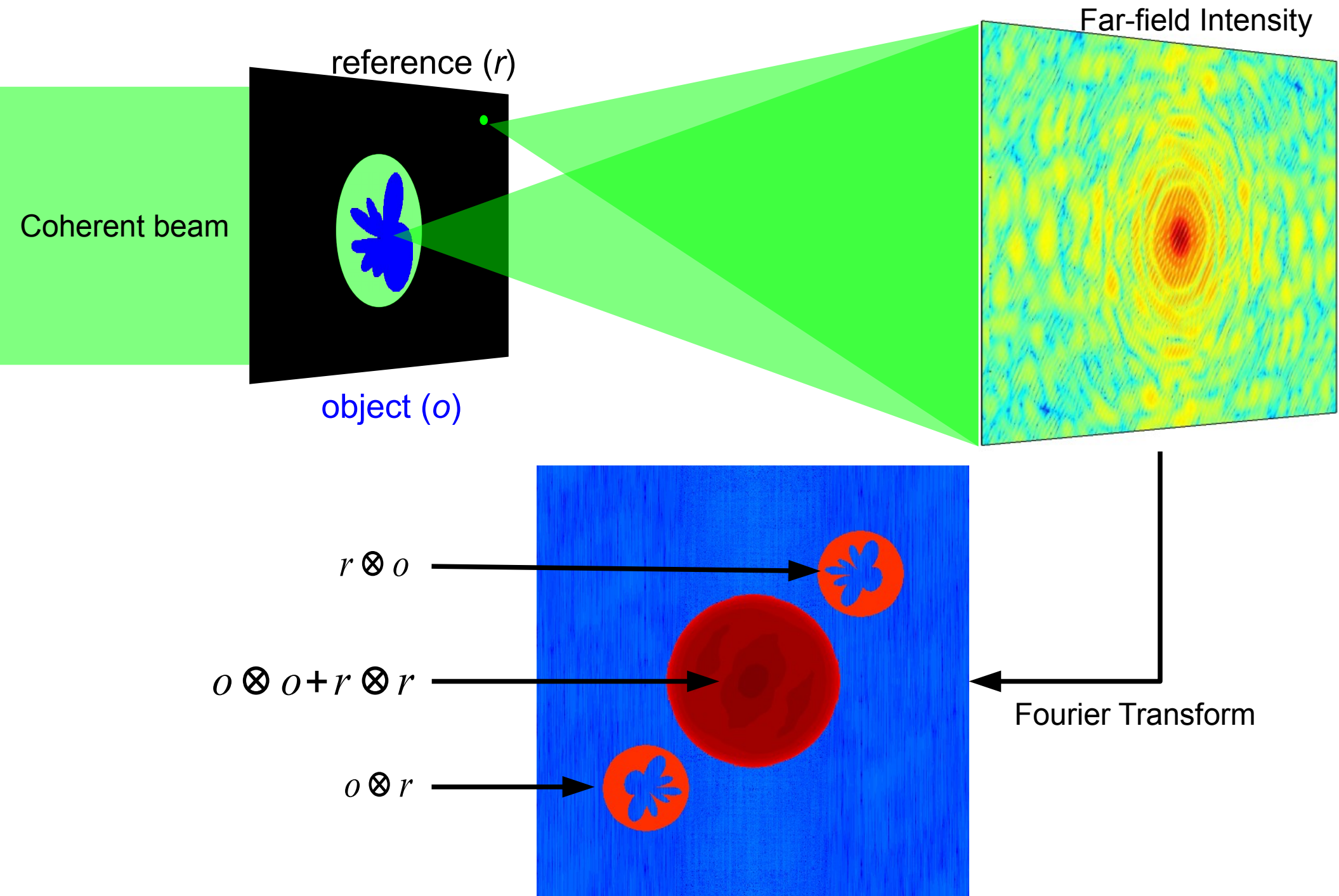
$$I(\mathbf{q}) = |\text{FT}\{f(\mathbf{r})\}|^2$$

Magnetic imaging – Fourier Transform Holography

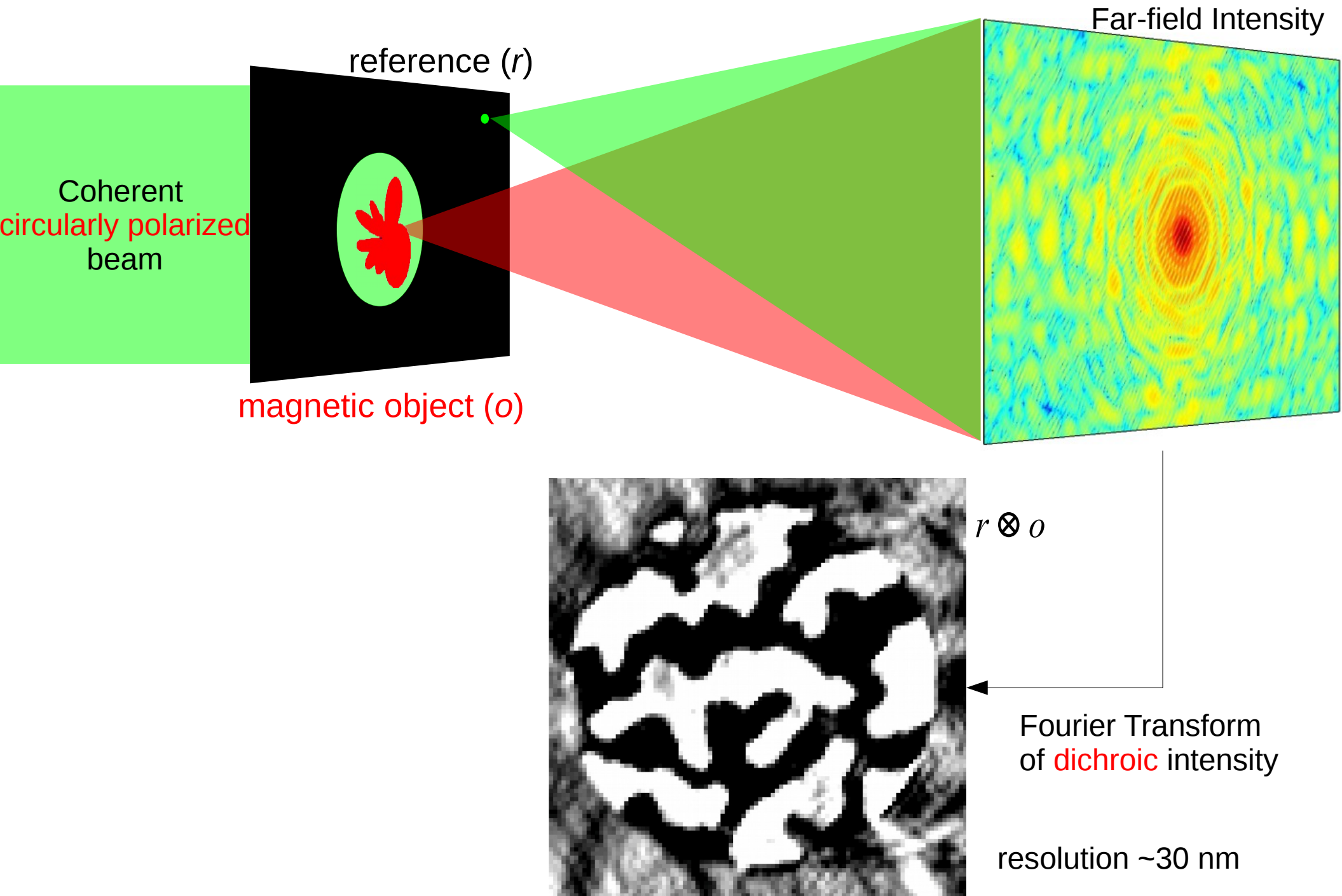
Eisebitt *et al*, Nature 2004



Magnetic imaging – Fourier Transform Holography



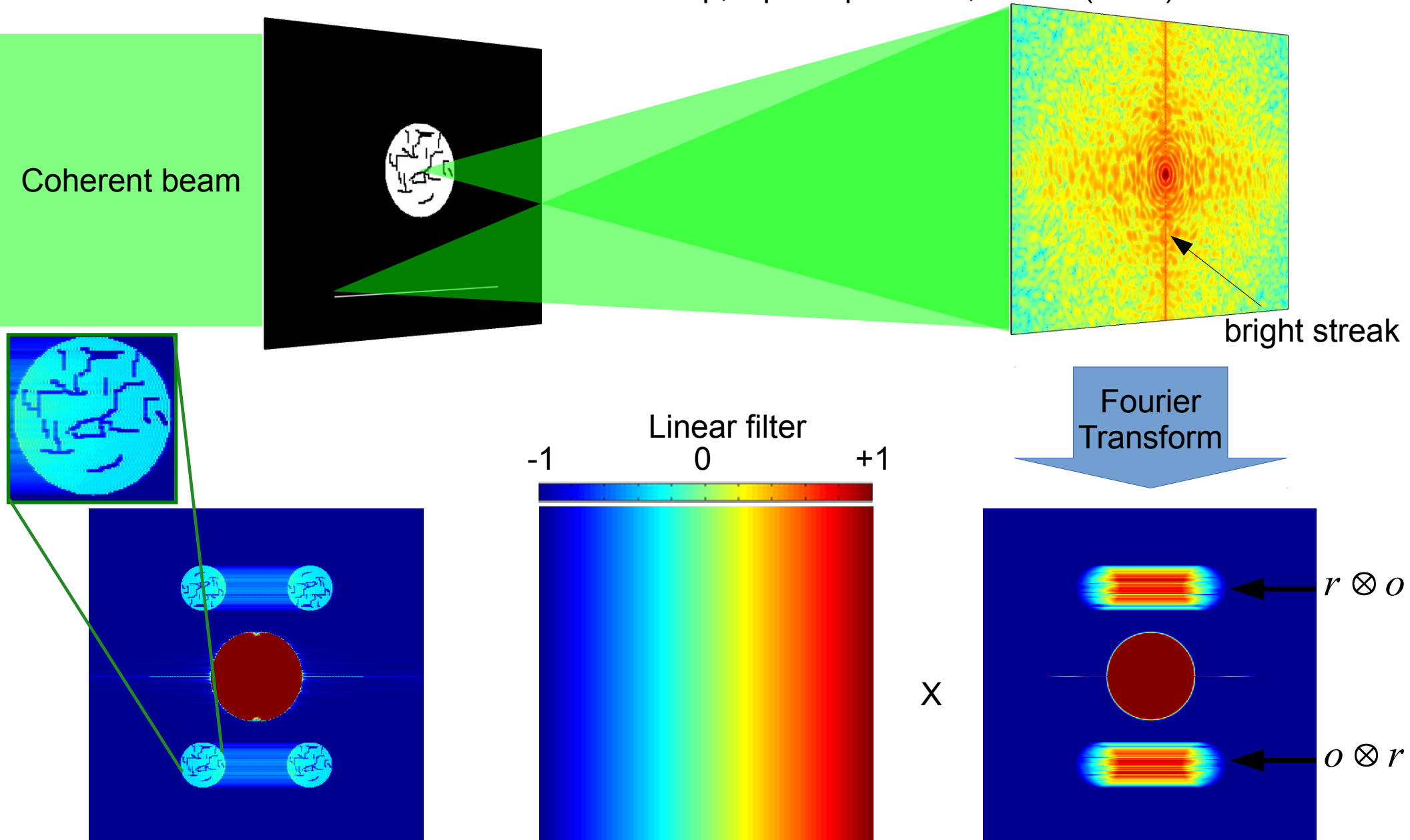
Magnetic imaging – Fourier Transform Holography



Magnetic imaging – Fourier Transform Holography

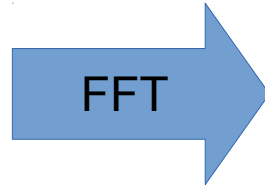
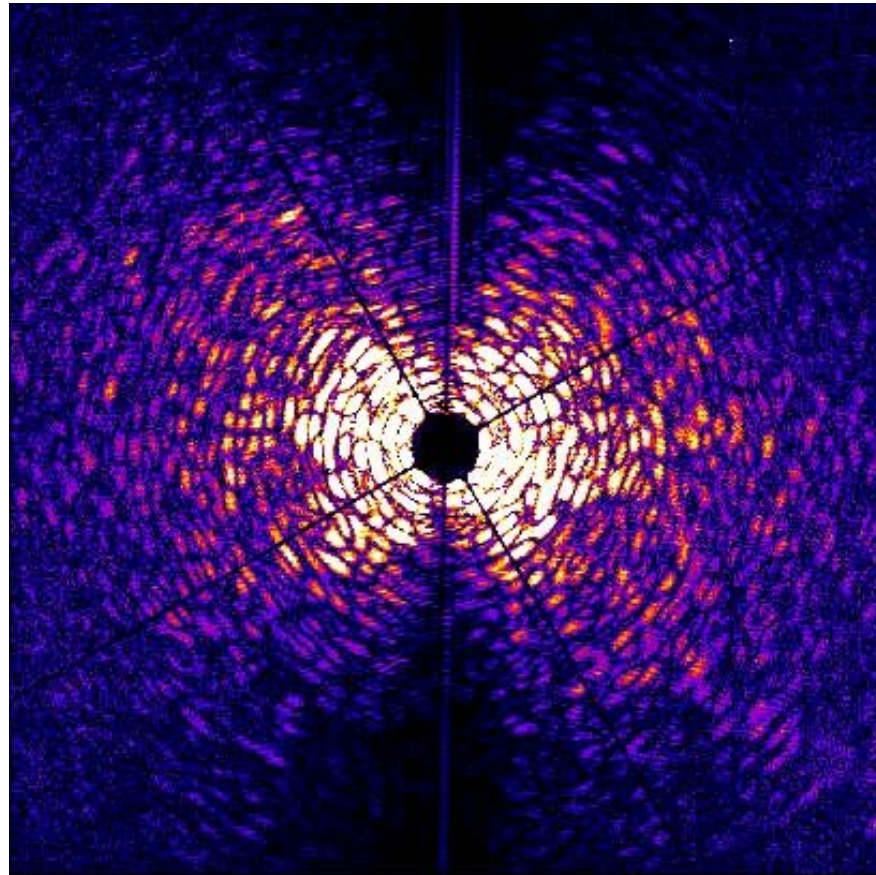
HERALDO

Holography with Extended Reference by Autocorrelation Linear Differential Operator
M. Guizar-Sicairos and J. R. Fienup, Opt. Express 15, 17592 (2007).

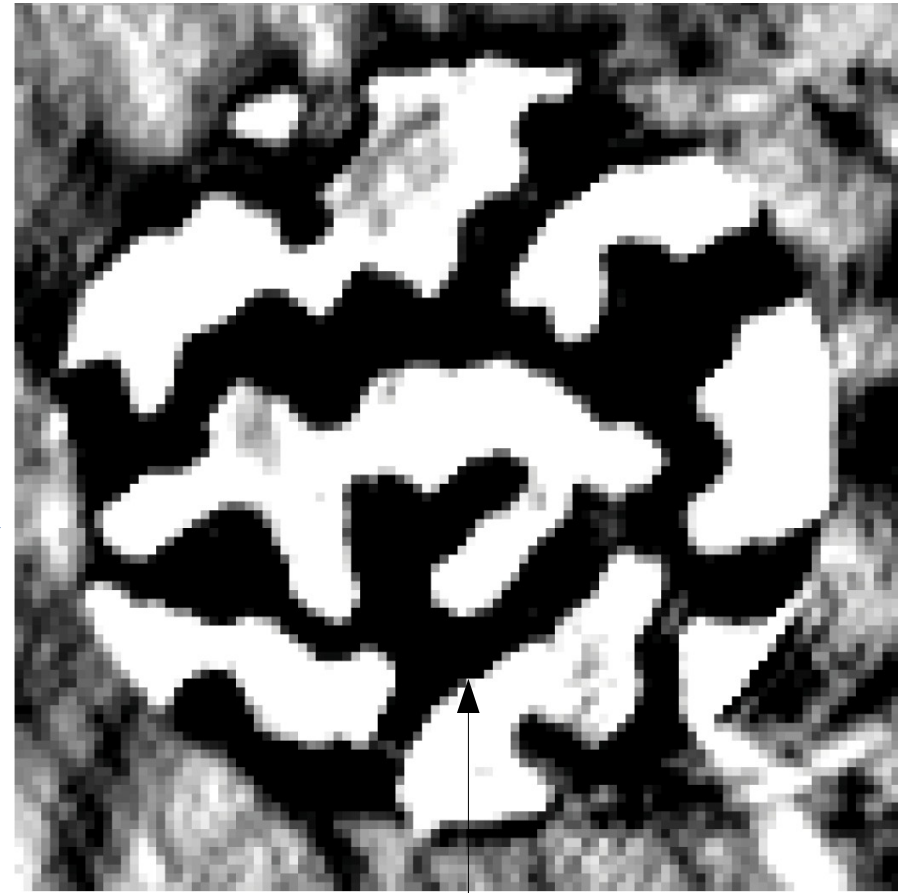


Magnetic imaging – Fourier Transform Holography

Hologram x Filter



Reconstructed image



Diamond I06, Co L3 edge

Resolution

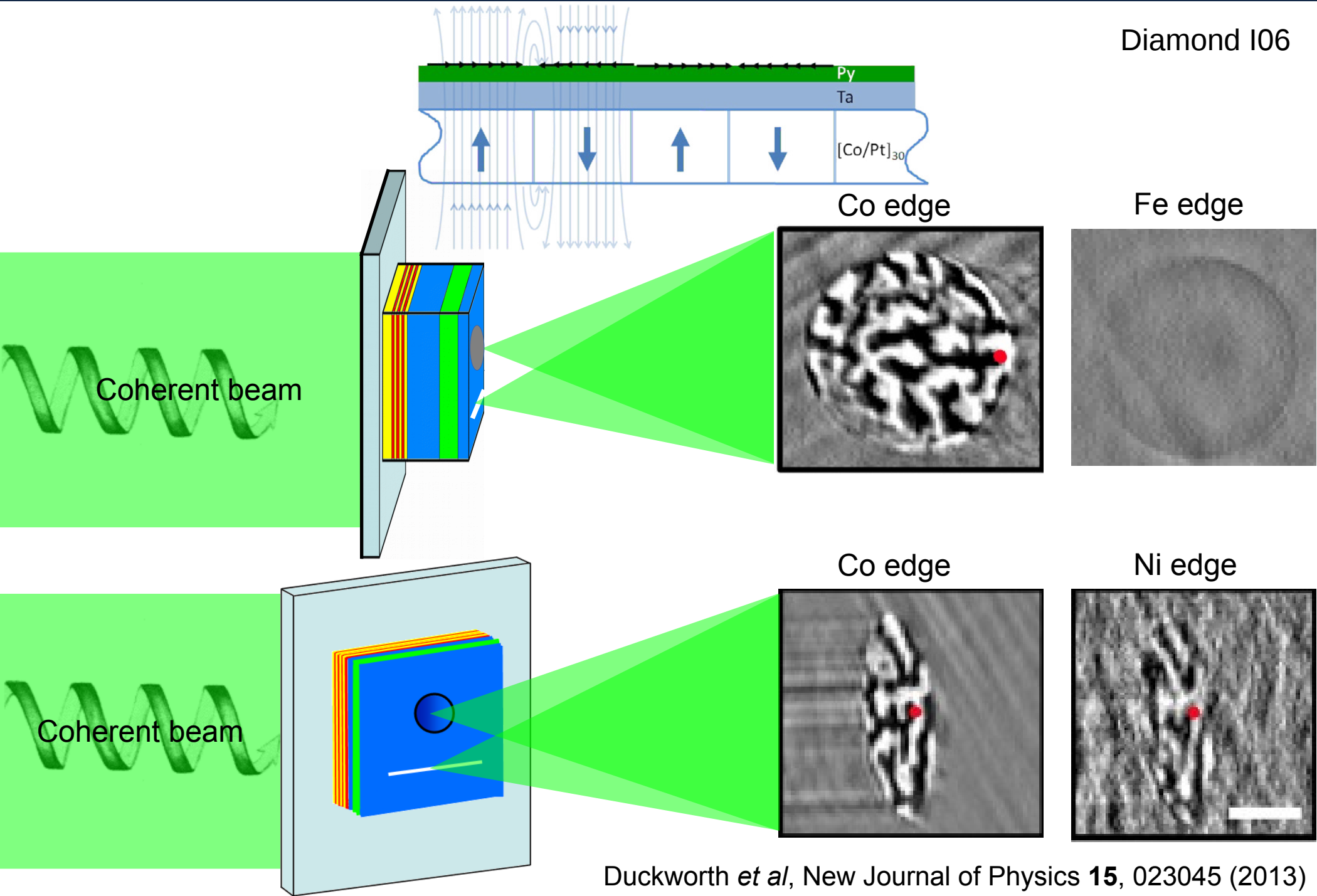
hole slit end



Domain walls sharper than resolution (~30 nm).
Resolution limited by CCD distance.

Duckworth *et al*, Optics Express **19**, 16223 (2011)

Magnetic imaging – Fourier Transform Holography



Duckworth *et al*, New Journal of Physics **15**, 023045 (2013)

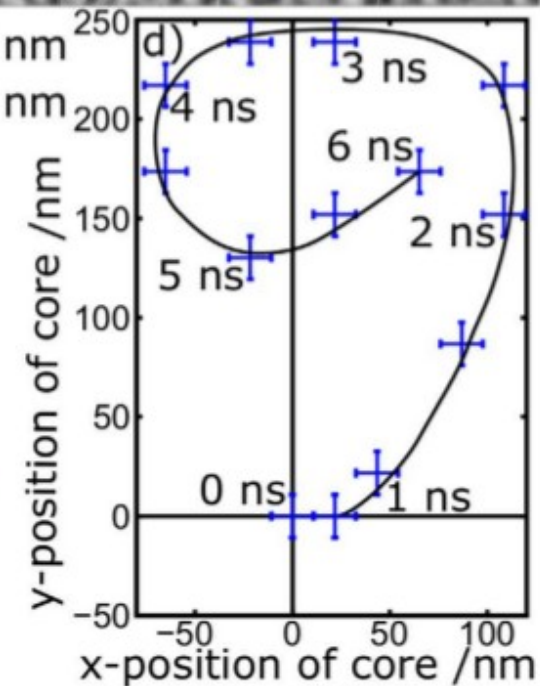
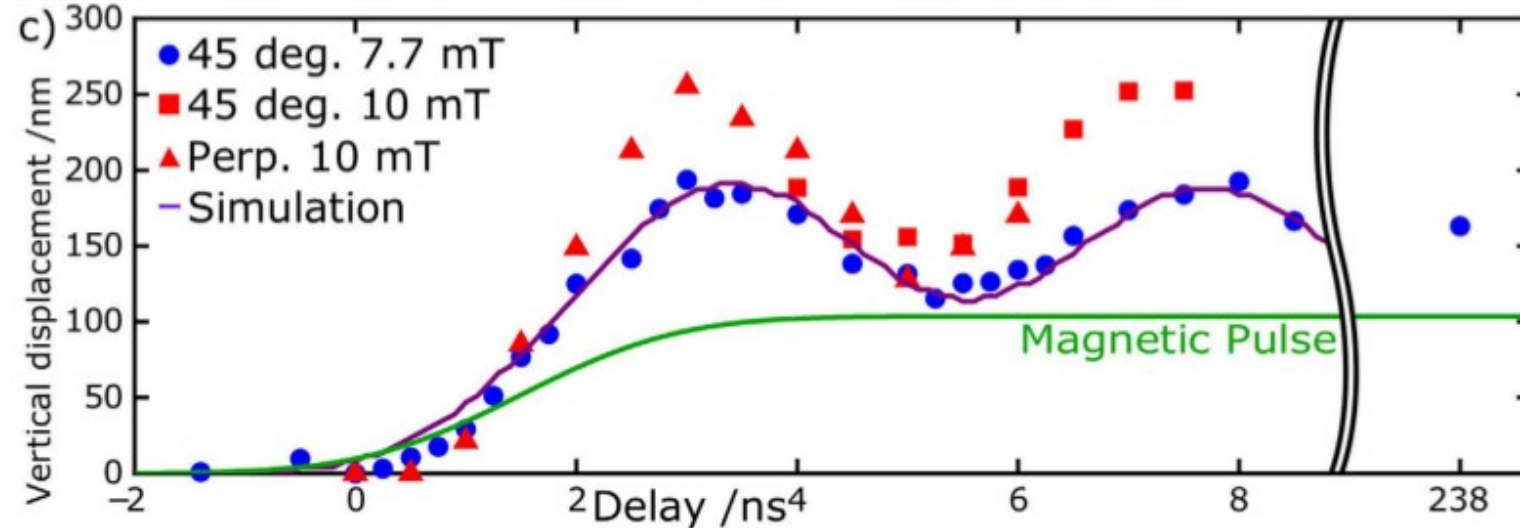
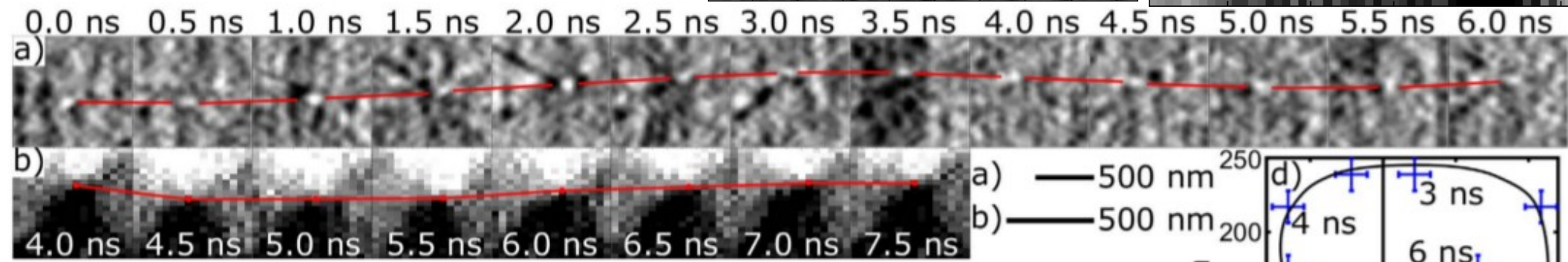
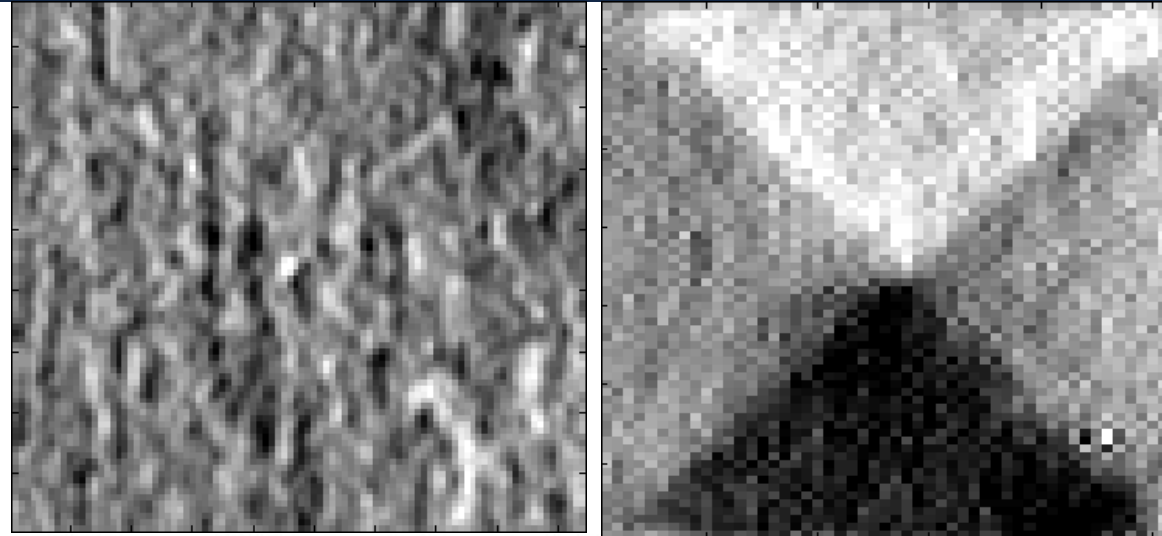
Magnetic imaging – Fourier Transform Holography

Soleil SEXTANTS & ESRF ID32

FeNi 2 μ m square element

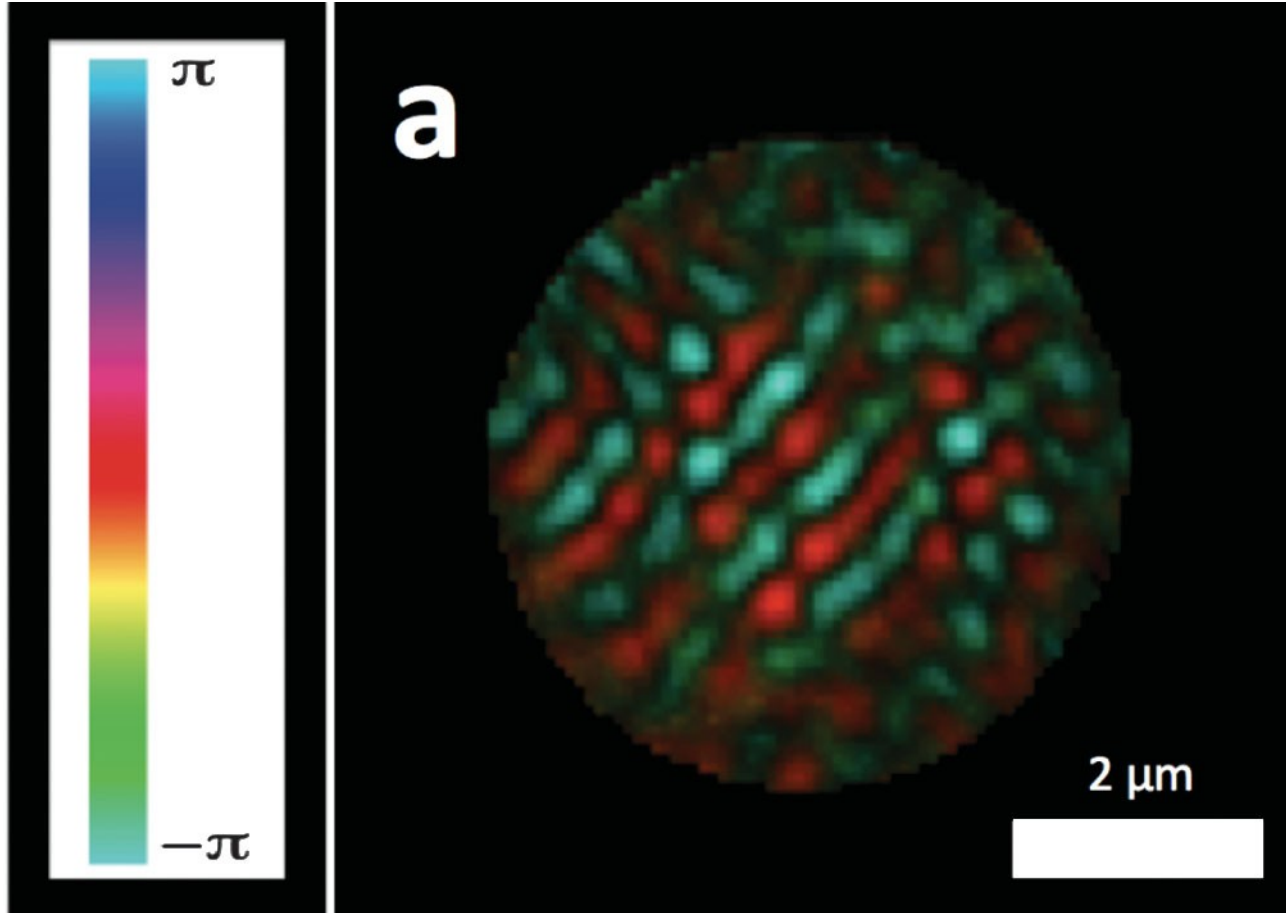
Fe L₃ edge (707 eV), resolution 20 nm

Bukin *et al*, Scientific Reports **6**, 36307 (2016)



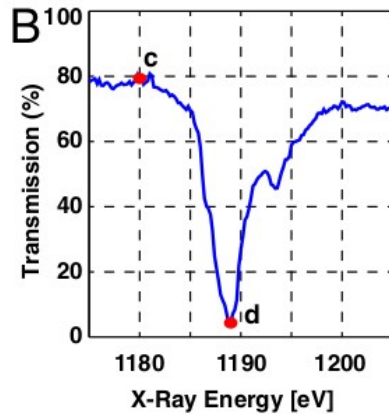
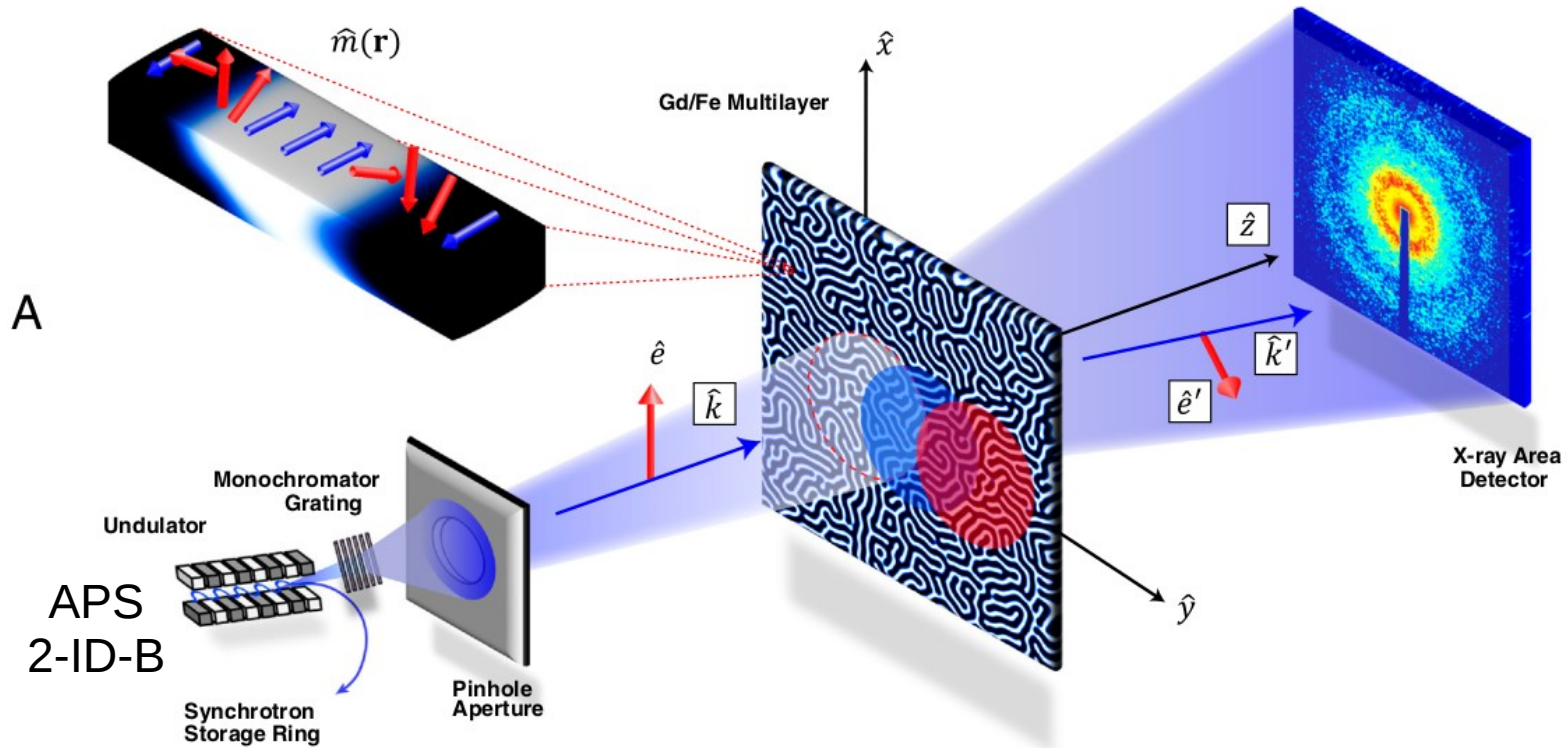
Magnetic imaging - CDI

TbCo film
Co L_3 edge (778 eV)
Linear polarisation, no polarisation analysis
Subtraction of saturated state (+normalisation)

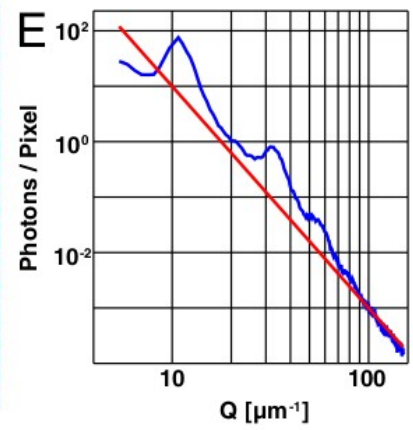
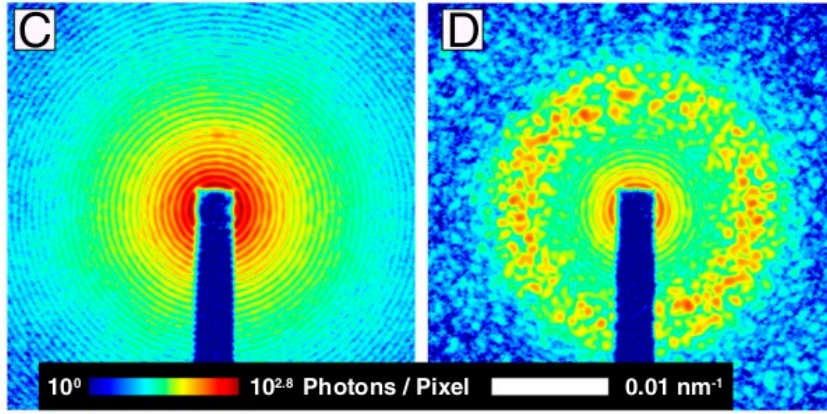


Turner *et al*, PRL 107, 033904 (2011)

Magnetic imaging - ptychography



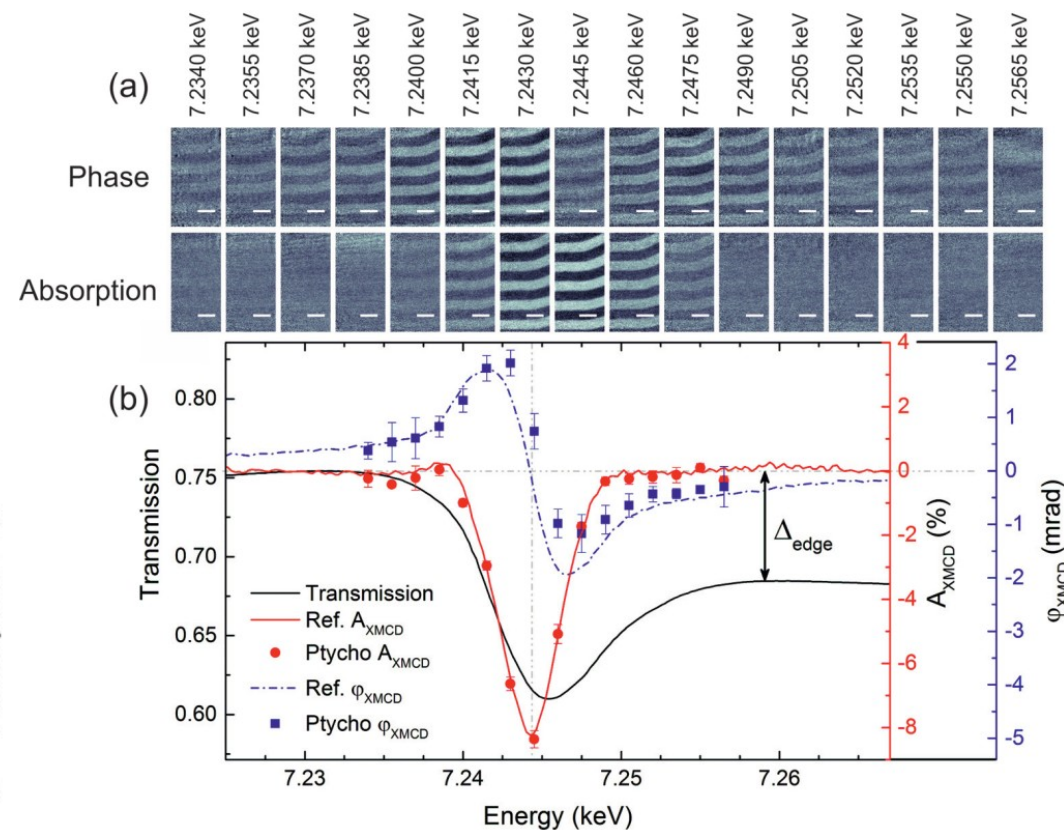
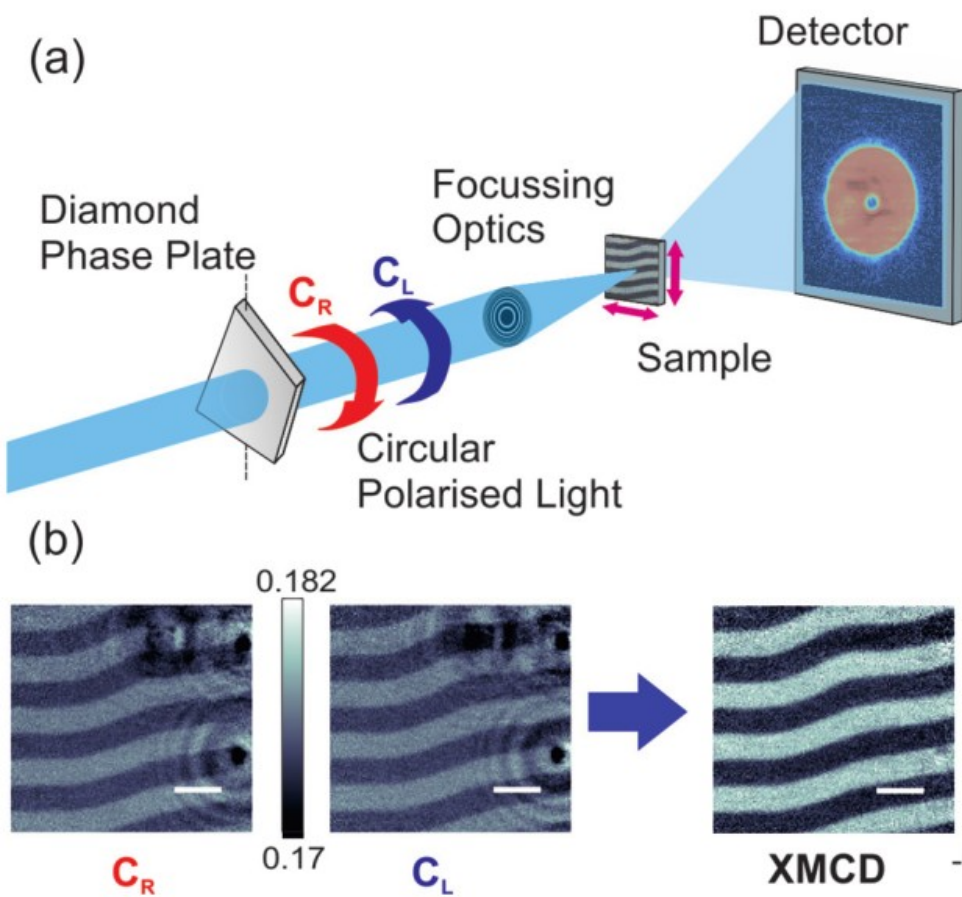
Gd M_5 edge



Tripathi *et al*, PNAS 108, 13397 (2011)

Magnetic imaging – ptychography (hard X-rays!)

FeGd multilayer, 1 μm thick, Gd L3 edge (7.243 keV) and Fe K edge (7.113 keV)



SLS cSAXS

Donnelly *et al*, Phys. Rev. B 94, 064421 (2016)

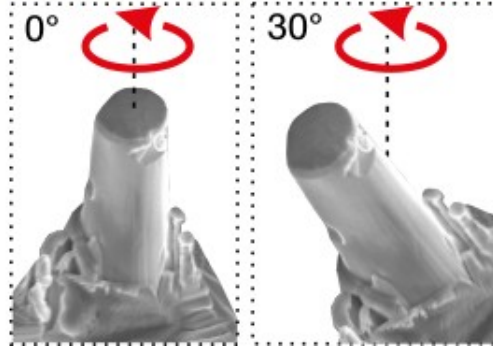
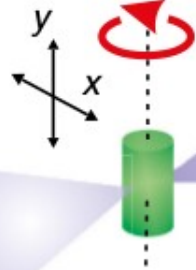
Magnetic imaging: ptychotomography

a

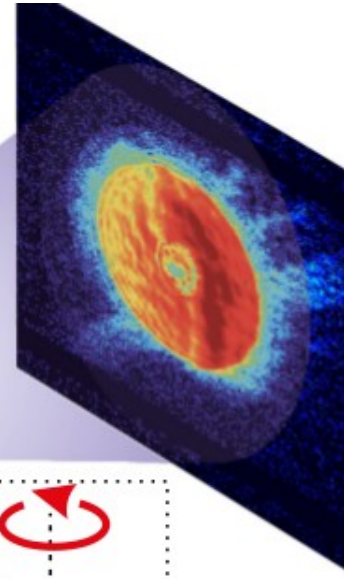
SLS cSAXS

Circularly polarized X-rays

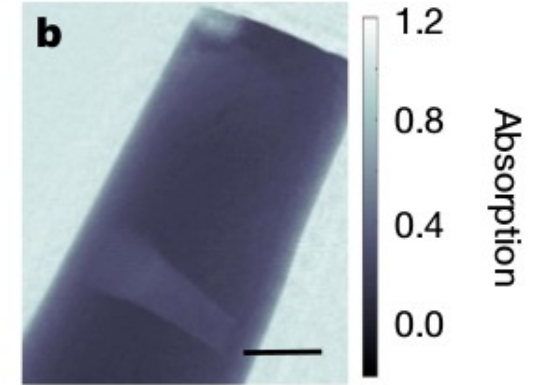
Optics



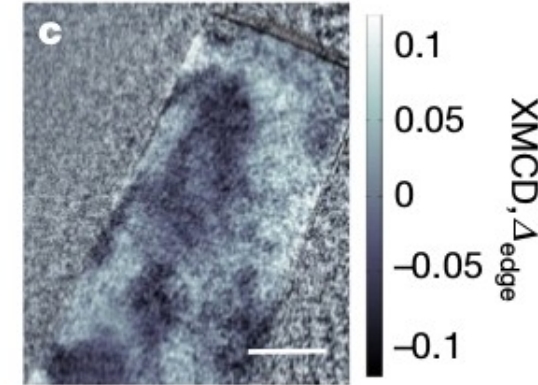
GdCo₂ cylinder of 5 μm diameter



b



c



Donnelly *et al*, Nature **547**, 328 (2017)

Magnetic imaging: towards 3D (tomography)

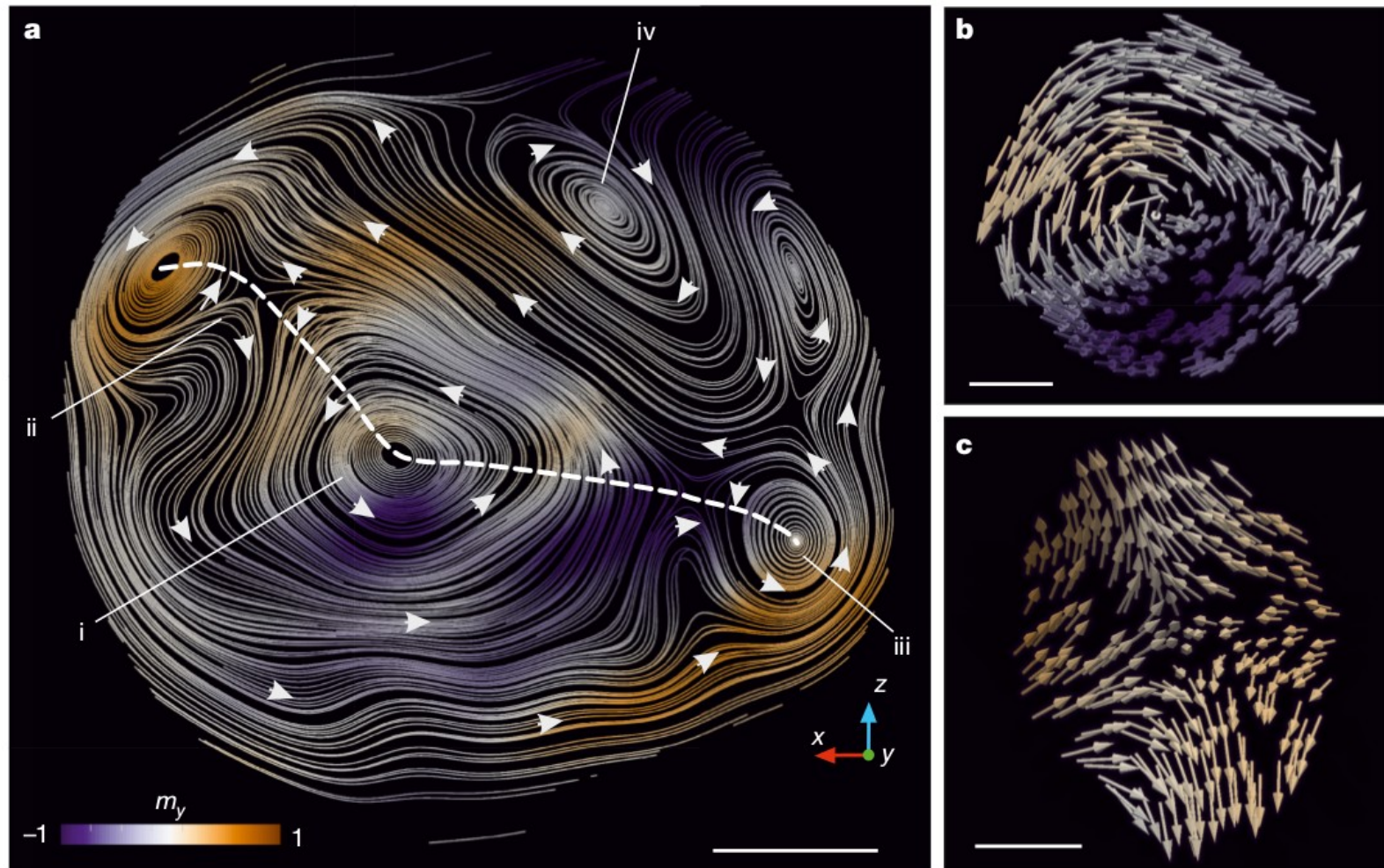
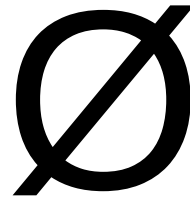


Figure 2 | Axial tomographic slice of the reconstructed magnetization vector field. **a**, A section taken perpendicular to the long axis of the cylindrical sample is shown, in which the streamlines represent the x - z components of the magnetization and different magnetic structures can be identified. There are anticlockwise vortices, such as (i) and (iii), a clockwise vortex (iv), and antivortices, such as (ii), which occur between

two vortices with the same vorticity. **b**, **c**, The three-dimensional magnetic nanostructure of vortex (i) and antivortex (ii), respectively, is shown in more detail. A section of a cross-tie wall consisting of a succession of vortex and antivortex structures is indicated by the dashed white line in **a**. Scale bars represent $1\ \mu\text{m}$ in **a** and $300\ \text{nm}$ in **b** and **c**.

Resolution on magnetic structure $\sim 100\ \text{nm}$

Donnelly *et al*, Nature **547**, 328 (2017)

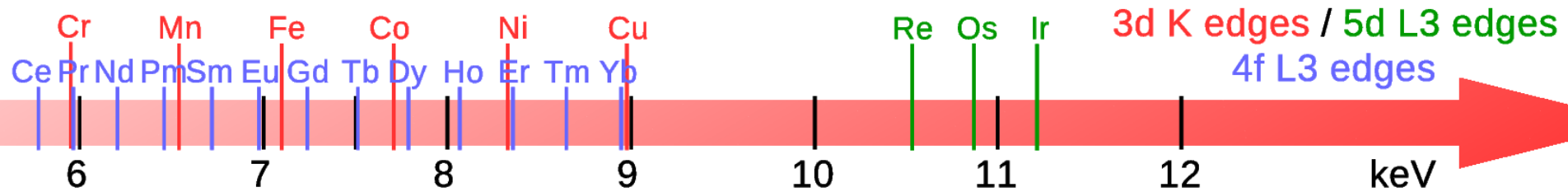


Bragg geometry → hard x-ray → weak magnetic signal
→ no ptychography (Bragg ptychography not a mature technique yet)

- **2D** imaging of **ferromagnetic** structures is achieved routinely using FTH (SAXS geometry) with **soft X-rays**
- **3D** imaging of **ferromagnetic** structures requires **hard X-rays** (because of penetration): has just been demonstrated (2017) on Rare-Earth material (ptychographic tomography in SAXS geometry)
- **2D/3D** imaging of **ANTIferromagnetic** structures requires **hard X-rays** (because of Bragg geometry): never done so far



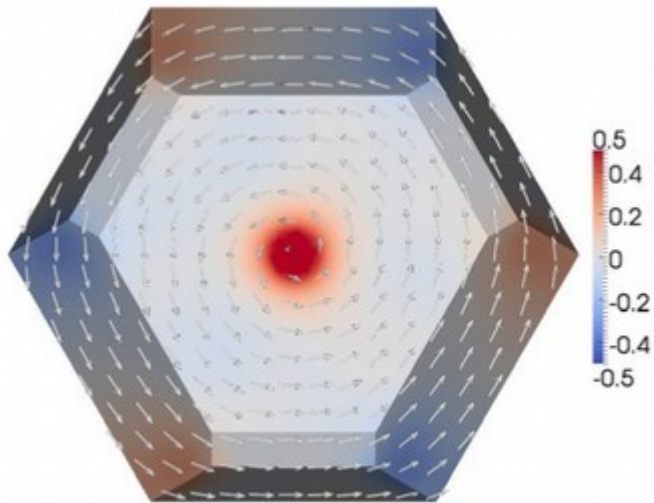
Perspectives with EBS



- Brilliance (B) x100 at 8 keV
- XPCS: Brilliance x100 $\rightarrow \tau / 10^4$
 - \rightarrow access to dynamics of magnetic systems with less pinning by structural defects
 - \rightarrow maybe dynamics of artificial spin ice?
- Coherent imaging:
 - \rightarrow improve resolution by ~ 3
 - \rightarrow 3D imaging with hard X-rays
 - \rightarrow antiferromagnetic systems (2D and 3D) with hard x-rays

3D view of ferromagnetic textures?

Geomagnetism / paleomagnetism



Effect of crystal strain and defects on magnetic structure in nanocrystals

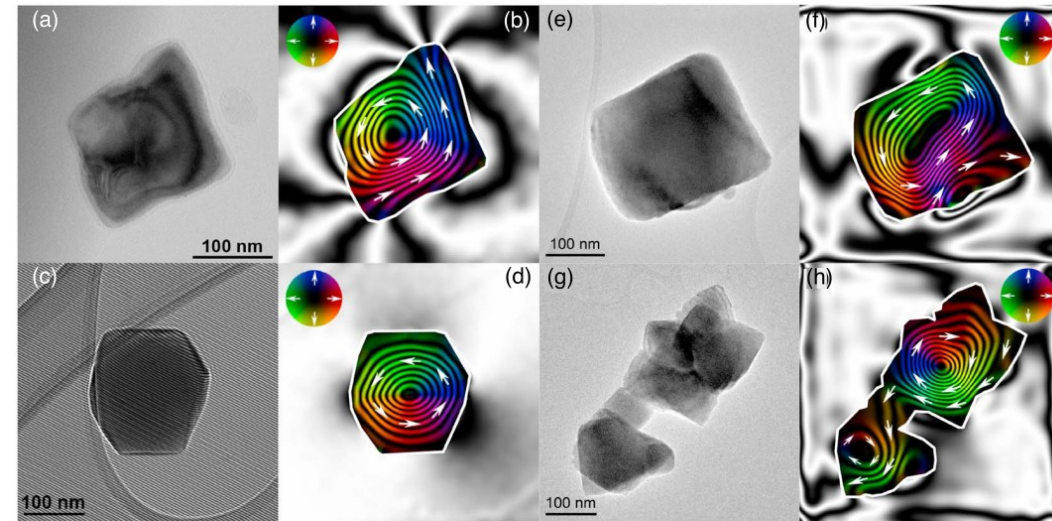
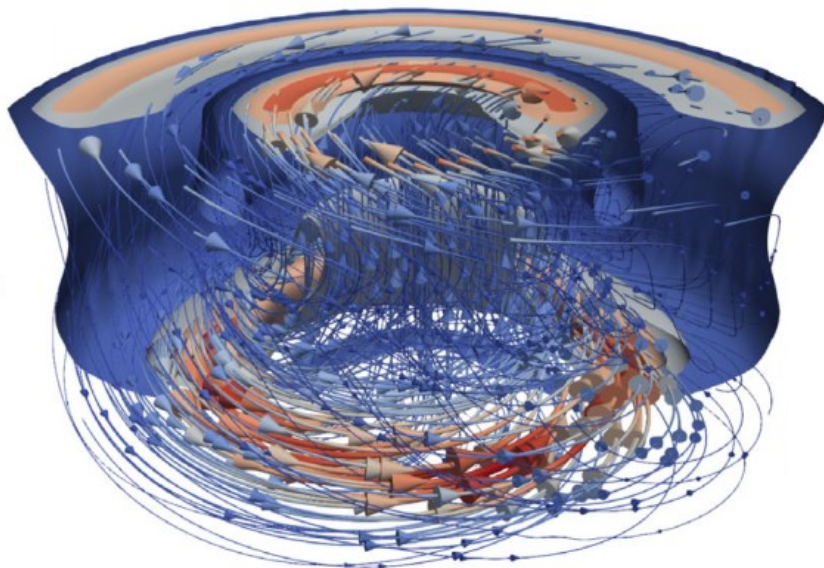


Figure 8. Electron holographic visualizations of single magnetic vortices in magnetite. (a) Bright-field TEM image of a particle ~ 250 nm in length. (b) Magnetic induction map reconstructed from electron holograms at room temperature (an in-plane saturating field was applied along the particle long axis to induce a remanent magnetization). (c and d) Electron hologram (with interference fringes used to calculate the magnetic contribution to the phase shift) and magnetic induction map for a hexagonal vortex state particle. Bright-field TEM image and induction map for a (e and f) single particle and (g and h) cluster of particles with nonvertically aligned vortex cores. All images are from the work of Almeida et al. (2016). The contour spacings (in radians) in the magnetic induction maps are 0.53 (Figure 8b), 0.78 (Figure 8d), 0.39 (Figure 8f), and 0.53 (Figure 8h); magnetization directions are indicated with arrows (depicted in the color wheels).

Skyrmions (2D) \rightarrow Hopf solitons (3D)

3D view of antiferromagnetic textures?

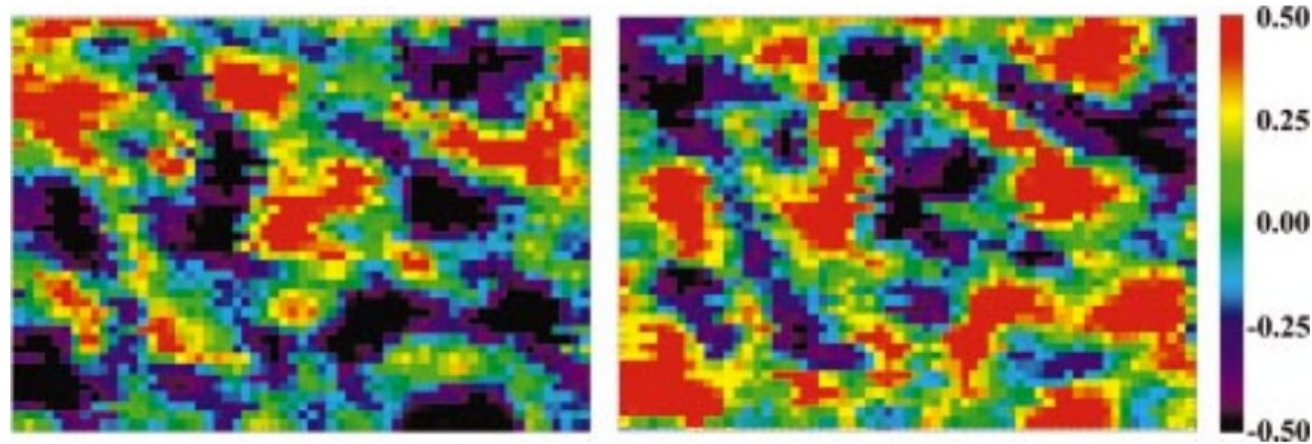
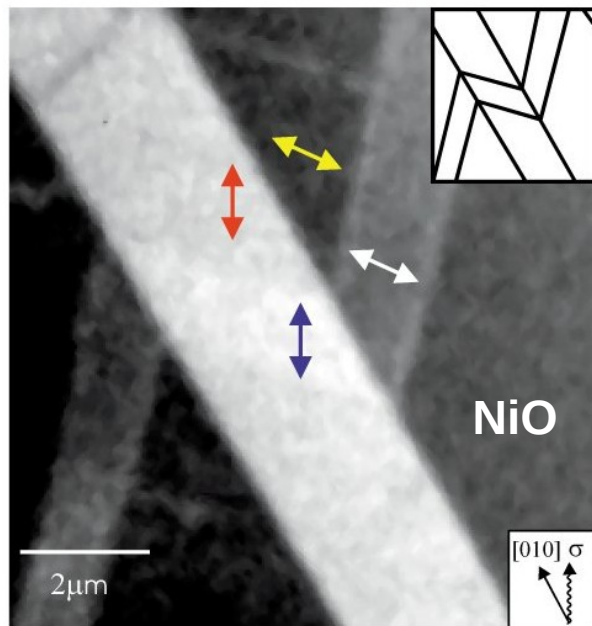


FIG. 5. (Color) Domain images ($600 \times 450 \mu\text{m}^2$) taken at the $-\tau$ (left) and $+\tau$ (right) magnetic peaks.



AFM materials:

- Visualisation of domains in bulk (including antiphase domains)
- Visualisation of phase slips in RE metals
- Relation structural defects / magnetic defects (cf. Le Bolloc'h)
- effect of nanoscale confinement?
- AFM/FM metamagnetic transition (FeRh): conservation of domains?

Thank you for your attention!

**We are looking for 2 students for PhD projects on coherent magnetic scattering!
Guillaume.beutier@grenoble-inp.fr**